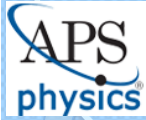


68th GEC
9th ICRP
33rd SPP
12-16 Oct. 15
Honolulu



Electron Scattering by biomass molecular fragments

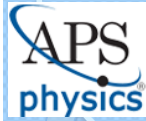
by
Marco A. P. Lima
Unicamp



1

MAPLima

68th GEC
9th ICRP
33rd SPP
12-16 Oct. 15
Honolulu



REVIEWING MOTIVATIONS



2

MAPLima

Electron scattering by Molecules

DISCHARGE ENVIROMENTS

This community was inspired by several basic science problems



and got further motivated by great applications



Natural Phenomena

Aurora Borealis

Astrophysics

Planetary Atmospheres

Biology

DNA dissociation ...
Plasma Science towards
Future Medicine

Quantum Optics

Molecular Lasers

Ozone destruction

Control of pollution

Sterilization \$\$

Surface treatment \$\$\$\$

Nanofabrication \$\$\$\$

Medical treatment \$\$\$\$

Surface treatment with Plasmas

Plasma
 Processing
 Gases

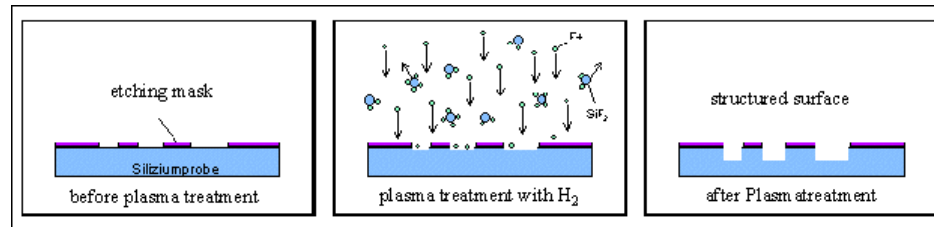


Several Industry Applications

Production
 of reactive
 species



ETCHING, DIAMANTIZATION,
 POLIMERIZATION, NITRIDING,
 CLEANING, and others



IMPROVEMENT NEEDS MODELING
 AND MODELING NEEDS DATA



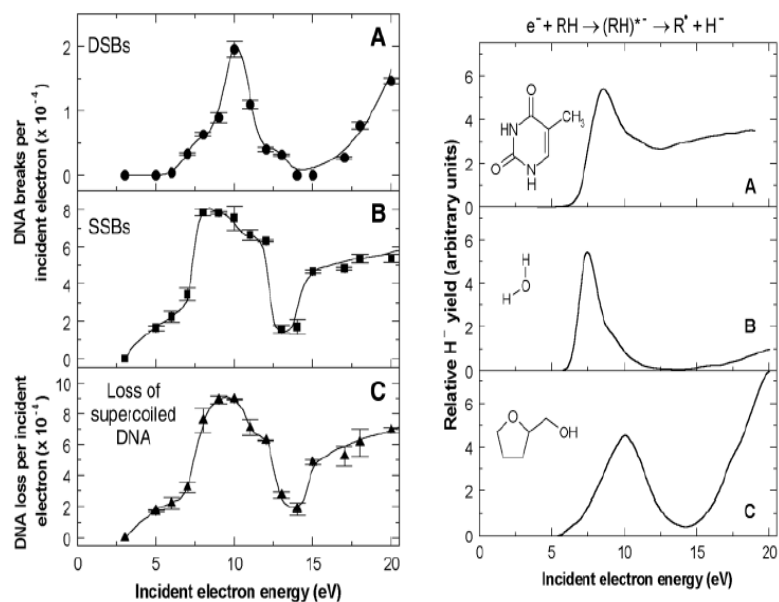
Electron collision
 data: cross
 sections for

Elastic
 Inelastic: **electronic, rotational and vibrational excitation**
 Ionization
 Dissociation

Electron-Induced Damage to Biomolecules

Resonant Formation of DNA Strand Breaks by Low-Energy (3 to 20 eV) Electrons

Badia Boudaïffa, Pierre Cloutier, Darel Hunting,
Michael A. Huels,* Léon Sanche



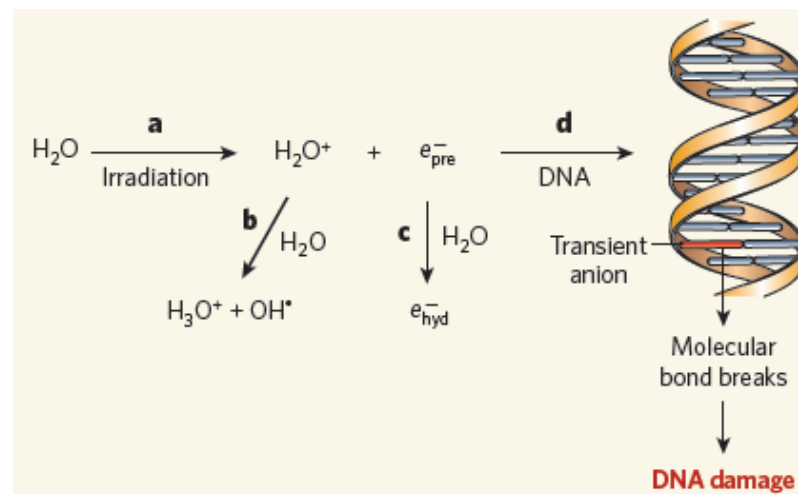
Science, **287** 1658 (2000)

BIOLOGICAL CHEMISTRY

Beyond radical thinking

Léon Sanche

Radiation-induced DNA damage has been attributed to hydroxyl radicals, which form when water absorbs high-energy photons or charged particles. But another product of water's radiolysis might be the real culprit.



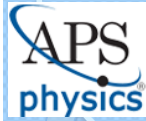
Sanche, Nature **461**, 358 (2009)

J|A|C|S
COMMUNICATIONS

Chun-Rong Wang, Jenny Nguyen, and Qing-Bin Lu*

J. AM. CHEM. SOC. 2009, **131**, 11320–11322

68th GEC
9th ICRP
33rd SPP
12-16 Oct. 15
Honolulu



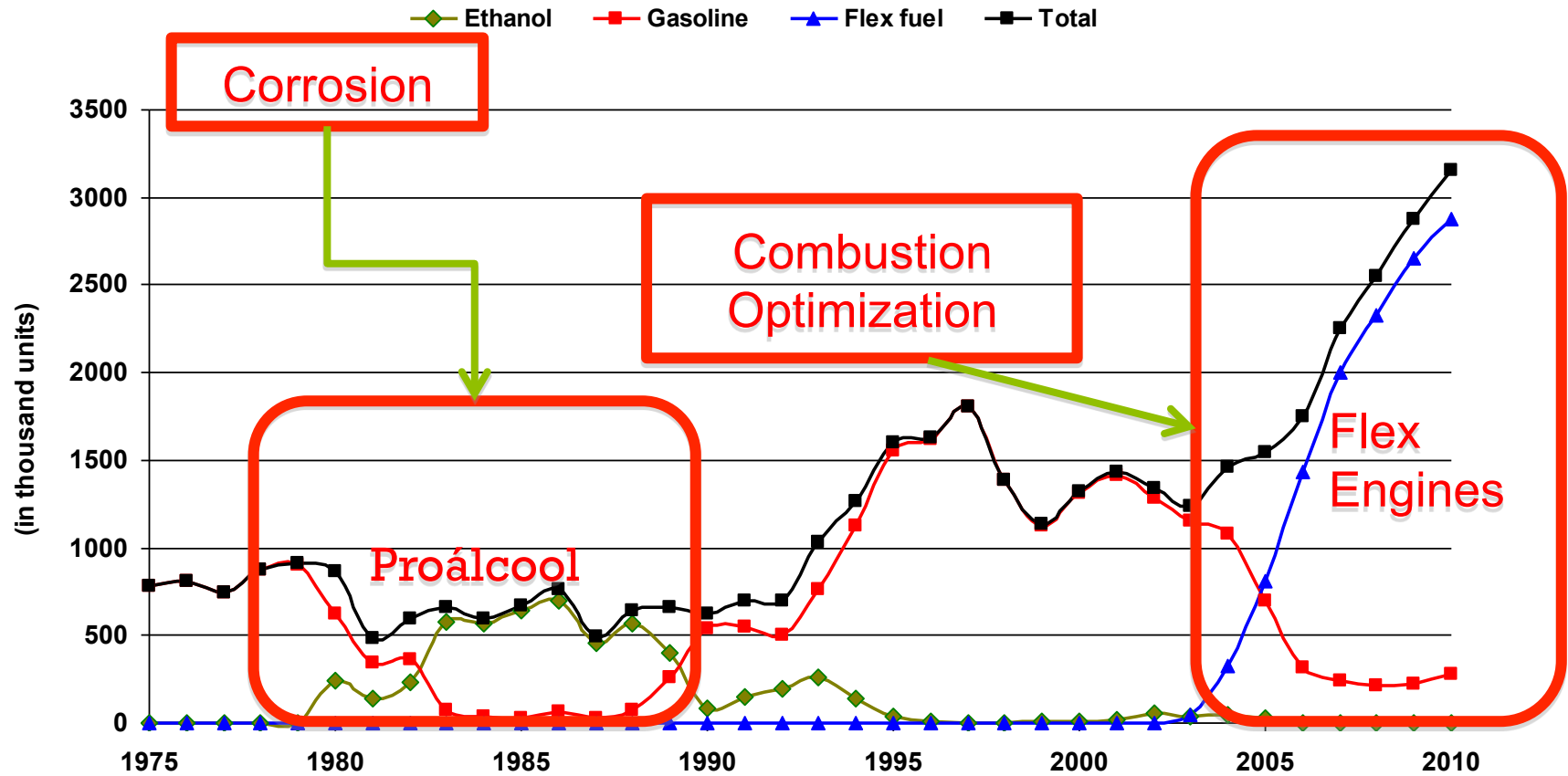
SPECIAL MOTIVATION



6

MAPLima

Special motivation I: large scale use of ethanol in engines



Brazilian Sales of light fleet Vehicles (1975-2010)

Ethanol as Fuel: Plasma Ignition for Vehicle Engines

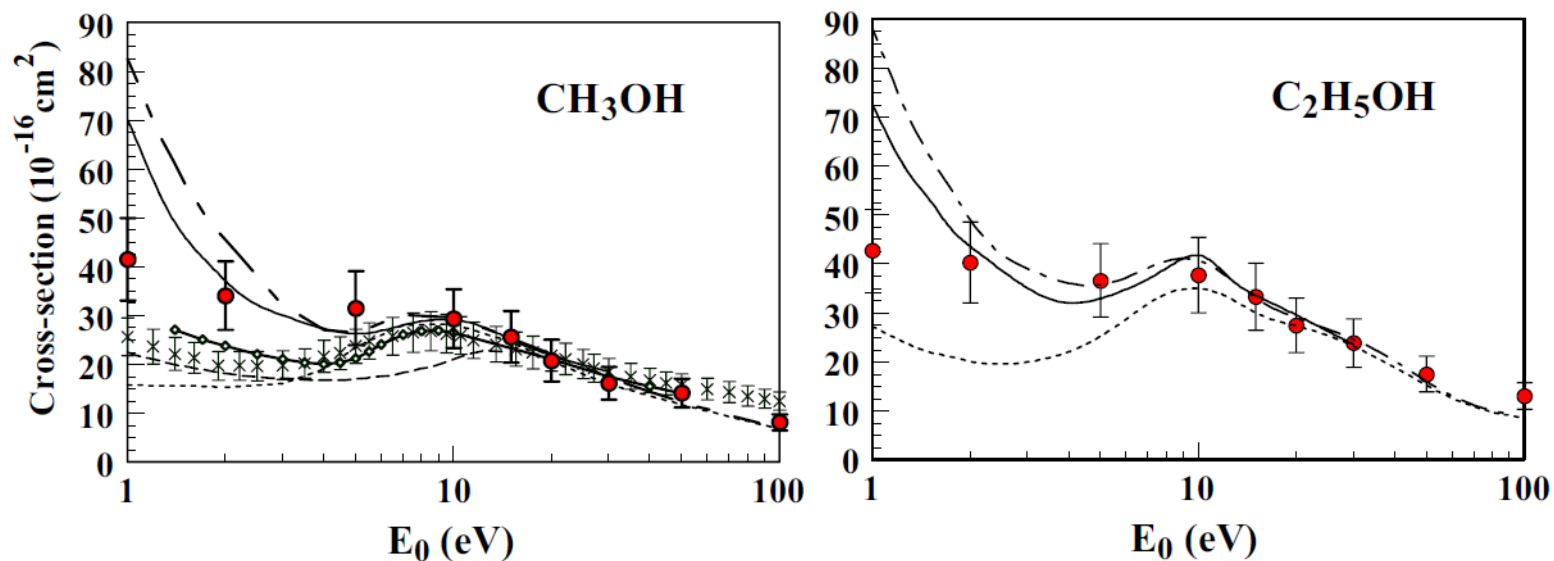


Theoretical support for an application project working on:

- Investigation of processes occurring during the ignition of plasma and its consequences in post-discharge for an internal combustion engine;
- The proper parameters to be applied in cars that operate on "poor mixtures" reducing pollutants released into the atmosphere, especially considering the spark plug discharge.

Low-energy elastic scattering from methanol and ethanol,

M.A. Khakoo, J. Blumer, K. Keane, C. Campbell, H. Silva, M. C.A. Lopes, C. Winstead, V. Mckoy, R. F. da Costa, L. G. Ferreira, M.A. P. Lima, and M. H. F. Bettega, *Phys. Rev. A* **77**, 042705 (2008).



Integral elastic scattering cross sections for CH₃OH. Legend: ●: present experiment; —: SMCPP SEP; —: SMC SEP; --- (short dashes): SMC SE which is similar to SMCPP SE; and ---- (long dashes): *R*-matrix ICSs of Bouchiha *et al.* (without Born correction) [10]. × Total cross section measurements of Szmytkowski and Krzysztofowicz [24] and —◆— of Schmiieder [22]. ---- (shortdashes) are from the SMCPP SE which is similar to SMC SE.

Other molecules like propanol, butanol and pentanol were also studied.

NSF (Caltech/Fullerton)/CNPq (Unicamp/UFJF/UFPR/USP/UFABC) project

Special motivation II: large scale production of ethanol



A sugarcane industry of Sugar/Ethanol/Bioelectricity

Special motivation II: large scale production of ethanol



Biomass: a source of energy and carbon

Special motivation II: large scale production of ethanol



Biomass: a source of energy and carbon

Special motivation II: large scale production of ethanol



First generation ethanol: crushing the cane for the juice

Special motivation II: large scale production of ethanol



**Bagasse piles
at the mill.**

**2nd generation
ethanol?
Other high value
bioproducts?**



Can we use plasmas on Biomass?

The motivation of a theoretician

➡ Scientific Challenge: in order to obtain reasonable results, it is necessary to learn how to control **APPROXIMATIONS** in many-body problems.

Scattering theory

See review: "Recent advances in the application of the Schwinger multichannel method with pseudopotentials to electron-molecule collisions", R. F. da Costa, M.T. do N. Varella, M.H.F. Bettega, and M.A.P. Lima, *Eur. Phys. J. D* **69**, I (2015).

Schrödinger equation

$$H\Psi_{\vec{k}_m}^{(\pm)}(\vec{r}_1, \dots, \vec{r}_{N+1}) = E\Psi_{\vec{k}_m}^{(\pm)}(\vec{r}_1, \dots, \vec{r}_{N+1})$$

Asymptotic condition

$$\Psi_{\vec{k}_i}^{(\pm)}(\vec{r}_1, \dots, \vec{r}_{N+1}) \xrightarrow{r_{N+1} \rightarrow \infty} S_{\vec{k}_i} + \sum_f^{\text{open}} f_{i \rightarrow f}^B(\vec{k}_i, \vec{k}_f) \Phi_f \frac{e^{\pm i k_f r_{N+1}}}{r_{N+1}}$$

$$S_{\vec{k}_i} = \Phi_i e^{i \vec{k}_i \cdot \vec{r}_{N+1}}$$

Differential cross section

$$\frac{d\sigma^{i \rightarrow f}}{d\Omega}(\vec{k}_i, \vec{k}_f) = \frac{k_f}{k_i} \left| f_{i \rightarrow f}^L(\vec{k}_i, \vec{k}_f) \right|^2$$

Scattering theory

Schrödinger differential equation

$$H\Psi_{\vec{k}_m}^{(\pm)} = [H_N + T_{N+1} + V]\Psi_{\vec{k}_m}^{(\pm)} = E\Psi_{\vec{k}_m}^{(\pm)}$$

Lippmann-Schwinger integral equation

$$\Psi_{\vec{k}_m}^{(\pm)} = S_{\vec{k}_m} + G_0^{(\pm)}V\Psi_{\vec{k}_m}^{(\pm)}$$

$$S_{\vec{k}_m} = \Phi_m e^{i\vec{k}_m \cdot \vec{r}_{N+1}}$$

Free-particle Green's function

$$G_0^{(\pm)} = \frac{1}{E - T_{N+1} - H_N \pm i\epsilon} = \lim_{\epsilon \rightarrow 0} \mathcal{P} \int d^3k \frac{|\Phi_m \vec{k}\rangle \langle \vec{k} \Phi_m|}{\frac{k_m^2}{2} - \frac{k^2}{2} \pm i\epsilon}$$

Schwinger Variational Principle

The Schwinger Variational method serves to get a scattering amplitude free of first order errors for a scattering process that respect the equations

$$A^{(\pm)}|\Psi_{\mathbf{k}}^{(\pm)}\rangle = V|S_{\mathbf{k}}\rangle \text{ and } \begin{cases} f_{\mathbf{k}_f, \mathbf{k}_i} = \langle S_{\mathbf{k}_f} | V | \Psi_{\mathbf{k}_i}^{(+)} \rangle \\ f_{\mathbf{k}_f, \mathbf{k}_i} = \langle \Psi_{\mathbf{k}_f}^{(-)} | V | S_{\mathbf{k}_i} \rangle \\ f_{\mathbf{k}_f, \mathbf{k}_i} = \langle \Psi_{\mathbf{k}_f}^{(-)} | A^{(+)} | \Psi_{\mathbf{k}_i}^{(+)} \rangle \end{cases} \quad \text{and } A^{(\pm)} = V - VG_0^{(\pm)}V$$

The bilinear form of the variational principle for the scattering amplitude is

$$[f_{\mathbf{k}_f, \mathbf{k}_i}] = \langle S_{\mathbf{k}_f} | V | \Psi_{\mathbf{k}_i}^{(+)} \rangle + \langle \Psi_{\mathbf{k}_f}^{(-)} | V | S_{\mathbf{k}_i} \rangle - \langle \Psi_{\mathbf{k}_f}^{(-)} | A^{(+)} | \Psi_{\mathbf{k}_i}^{(+)} \rangle \text{ where arbitrary and}$$

independent variations with respect to

$$\begin{cases} \langle \delta \Psi_{\mathbf{k}_f}^{(-)} | (V | S_{\mathbf{k}_i} \rangle - A^{(+)} | \Psi_{\mathbf{k}_i}^{(+)} \rangle) = 0 \\ (\langle S_{\mathbf{k}_f} | V - \langle \Psi_{\mathbf{k}_f}^{(-)} | A^{(+)} \rangle) | \delta \Psi_{\mathbf{k}_i}^{(+)} \rangle = 0 \end{cases}$$

lead to

$$\begin{cases} V | S_{\mathbf{k}_i} \rangle - A^{(+)} | \Psi_{\mathbf{k}_i}^{(+)} \rangle = 0 \Rightarrow A^{(+)} | \Psi_{\mathbf{k}_i}^{(+)} \rangle = V | S_{\mathbf{k}_i} \rangle \\ \langle S_{\mathbf{k}_f} | V - \langle \Psi_{\mathbf{k}_f}^{(-)} | A^{(+)} = 0 \Rightarrow A^{(-)} | \Psi_{\mathbf{k}_f}^{(-)} \rangle = V | S_{\mathbf{k}_f} \rangle \text{ with } A^{(+)\dagger} = A^{(-)} \end{cases}$$

$A^{(\pm)}|\Psi_{\mathbf{k}}^{(\pm)}\rangle = V|S_{\mathbf{k}}\rangle$ is equivalent to $H|\Psi_{\mathbf{k}}^{(\pm)}\rangle = E|\Psi_{\mathbf{k}}^{(\pm)}\rangle$ with proper boundary conditions.

Schwinger Multichannel Method for electron scattering

In this formalism the operator $A^{(+)}$ was redefined as:

$$A^{(+)} = \frac{1}{2}(PV + VP) - VG_P^{(+)}V + \frac{1}{N+1} \left[\hat{H} - \frac{N+1}{2}(\hat{H}P + P\hat{H}) \right]$$

where $P \equiv \sum_{\ell=1}^{\text{open}} |\Phi_{\ell}\rangle\langle\Phi_{\ell}|$ and $\hat{H} = E - H$

All electrons are identical. So, an expansion of the scattering wave function must be done in a basis $\{\chi_{\mu}\}$ of anti-symmetric functions (Slater determinants):

$$|\Psi_{\vec{k}_m}^{(\pm)}\rangle = \sum_{\mu} a_{\mu}^{(\pm)}(\vec{k}_m) |\chi_{\mu}\rangle \quad \text{where} \quad \{|\chi_{\mu}\rangle\} = \{\mathbf{a}_{N+1} |\Phi_i\rangle \otimes |\varphi_j\rangle\}$$

The final form of the scattering amplitude is equal to the one of the Schwinger Variational principle

$$f_{\vec{k}_i, \vec{k}_f} = -\frac{1}{2\pi} \sum_{mn} \langle S_{\vec{k}_f} | \underbrace{V |\chi_m\rangle (d^{-1})_{mn} \langle \chi_n | V | S_{\vec{k}_i}} \rangle$$

It is the same for all transitions

with $d_{mn} = \langle \chi_m | A^{(+)} | \chi_n \rangle$ and $S_{\vec{k}_i} \equiv \Phi_i(\vec{r}_1, \dots, \vec{r}_N) e^{i\vec{k}_i \cdot \vec{r}_{N+1}}$

Coupling level

➔ Elastic scattering with and without polarization effects

① Open channel Projector has only one state

$$P = |\Phi_0\rangle\langle\Phi_0| \quad \Rightarrow$$

Φ_0 is molecular target ground state obtained in Hartree-Fock approximation

② Configuration space is made of

$$|\chi_\mu\rangle = \begin{cases} a_{N+1} |\Phi_0\rangle \otimes |\varphi_i\rangle \\ a_{N+1} |\Phi_j\rangle \otimes |\varphi_k\rangle, j \geq 2 \end{cases} \quad \Rightarrow$$

Doublet states made of products of target triplet and singlet states by φ_k

➔ $\Phi_j, j \geq 2$ are virtual states obtained from single excitations of the molecular target

➔ φ_i are one-particle wave functions (square integrable molecular orbitals) used in description of the continuum

Coupling level

➡ Inelastic scattering with and without polarization

- 1 Open channel projector contains channels of our choice (truncation means approximation)

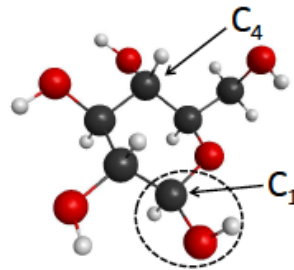
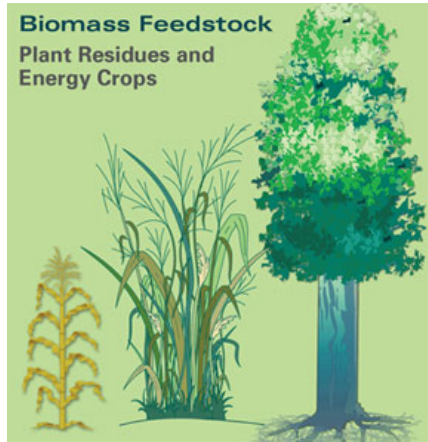
$$P = \sum_{\ell}^{\text{open}} |\Phi_{\ell}\rangle \langle \Phi_{\ell}| \quad \Rightarrow \quad |\Phi_{\ell}\rangle \text{ are molecular target states obtained with single configuration interaction}$$

- 2 Again the configuration space is made of

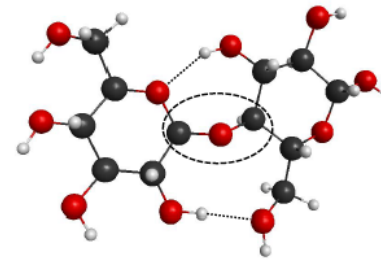
$$|\chi_{\mu}\rangle = \begin{cases} \mathbf{a}_{N+1} |\Phi_0\rangle \otimes |\varphi_i\rangle \\ \mathbf{a}_{N+1} |\Phi_j\rangle \otimes |\varphi_k\rangle, j \geq 2 \end{cases} \quad \Rightarrow \quad \text{Doublet states made of products of target triplet and singlet states by } \varphi_k$$

- ➡ Polarization effects are included with j greater than the number of open channels

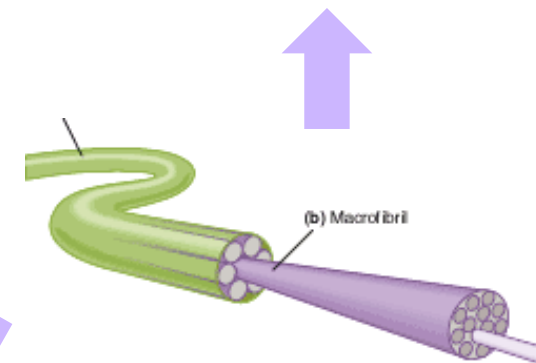
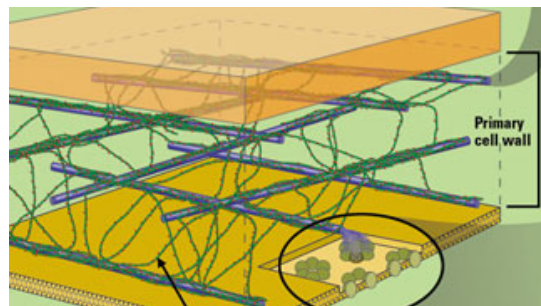
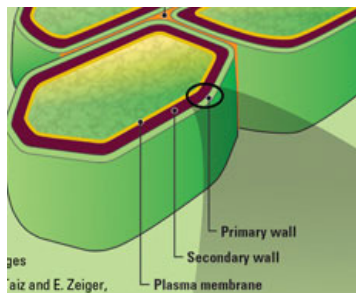
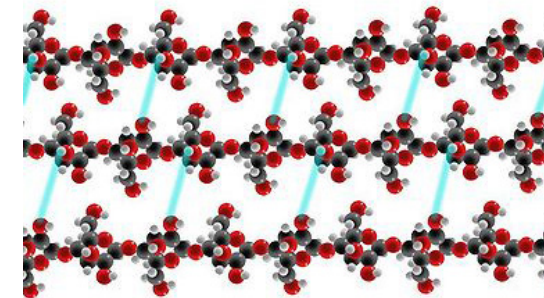
Biomass is Made Up with Fermentable Sugars



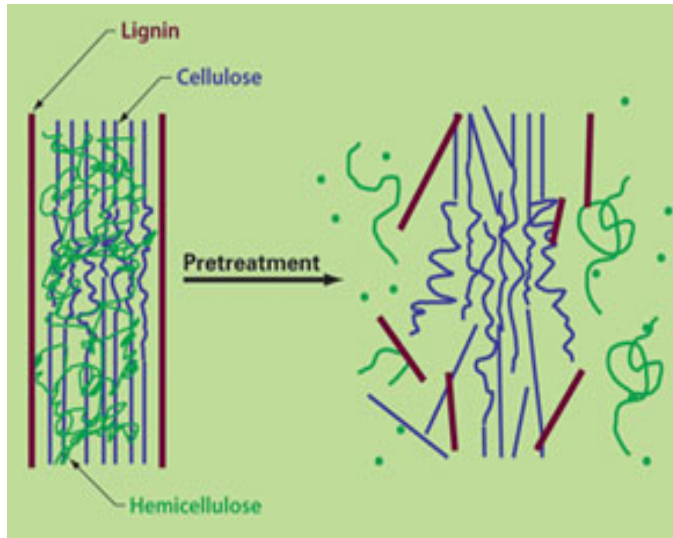
β -D-glucose



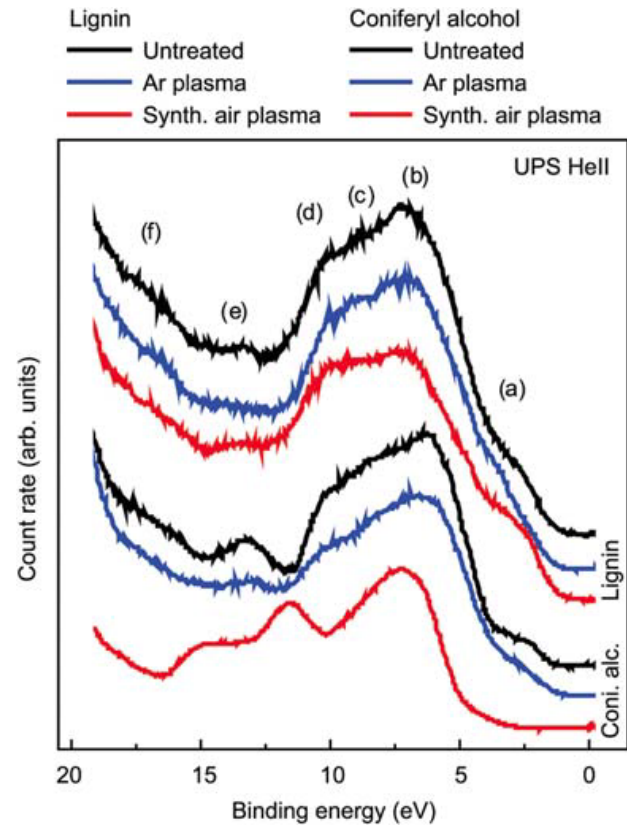
cellobiose



Lignocellulose is Resistant to Hydrolysis



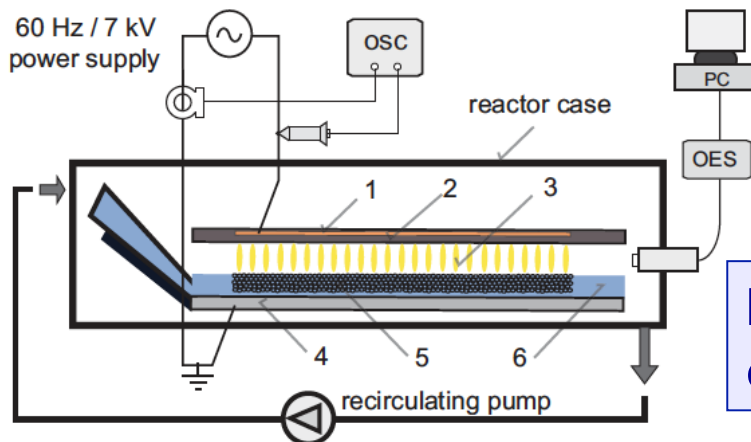
Pretreatment: bio- and physical-chemical processes to expose the cellulose fibers



Lothar Klarhöfer¹, Wolfgang Viöl^{2,3,*} and Wolfgang Maus-Friedrichs¹

Holzforschung, Vol. 64, pp. 331–336, 2010

**Dielectric Barrier Discharge (DBD):
 electron flux on substrate $\sim 10^8 \text{ cm}^{-2} \text{ s}^{-1}$**





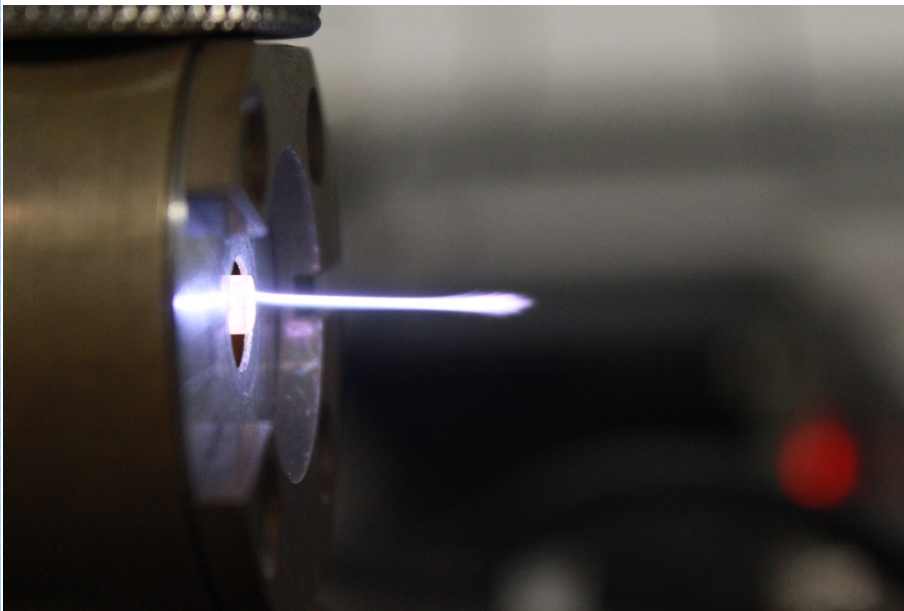
Experimental Initiative



supported by



- Microwave Plasmas in argon at atmospheric pressure
- Exploration of their potential for applications, in particular, to the treatment of biomass (sugar cane bagasse)



By Jayr Amorim, Carlos Oliveira, Jorge A. Souza-Correa, Marco A. Ridenti
Plasma Process. Polym. 2013, DOI: 10.1002/ppap.201200158



Diffuse Reflectance Fourier Transform Infrared Spectrometry (DRIFT)



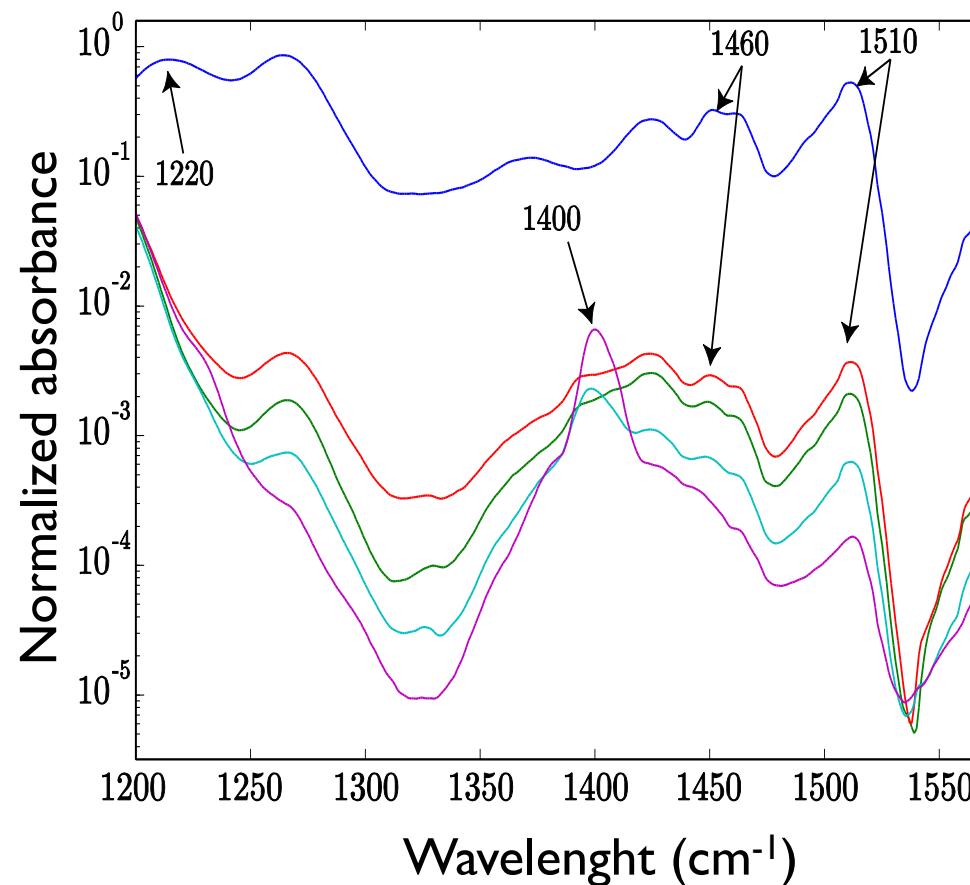
wavelength:

➔ **1220 cm⁻¹**

CC plus CO plus CO
stretching in Guaiacyl group

➔ **1460 cm⁻¹**

CH deformations (bend)
methoxyl; asymmetric
stretching in -CH₃ and -CH₂



(—) not treated (—) 0.5h (—) 1 h; (—) 2 h; (—) 4 h.

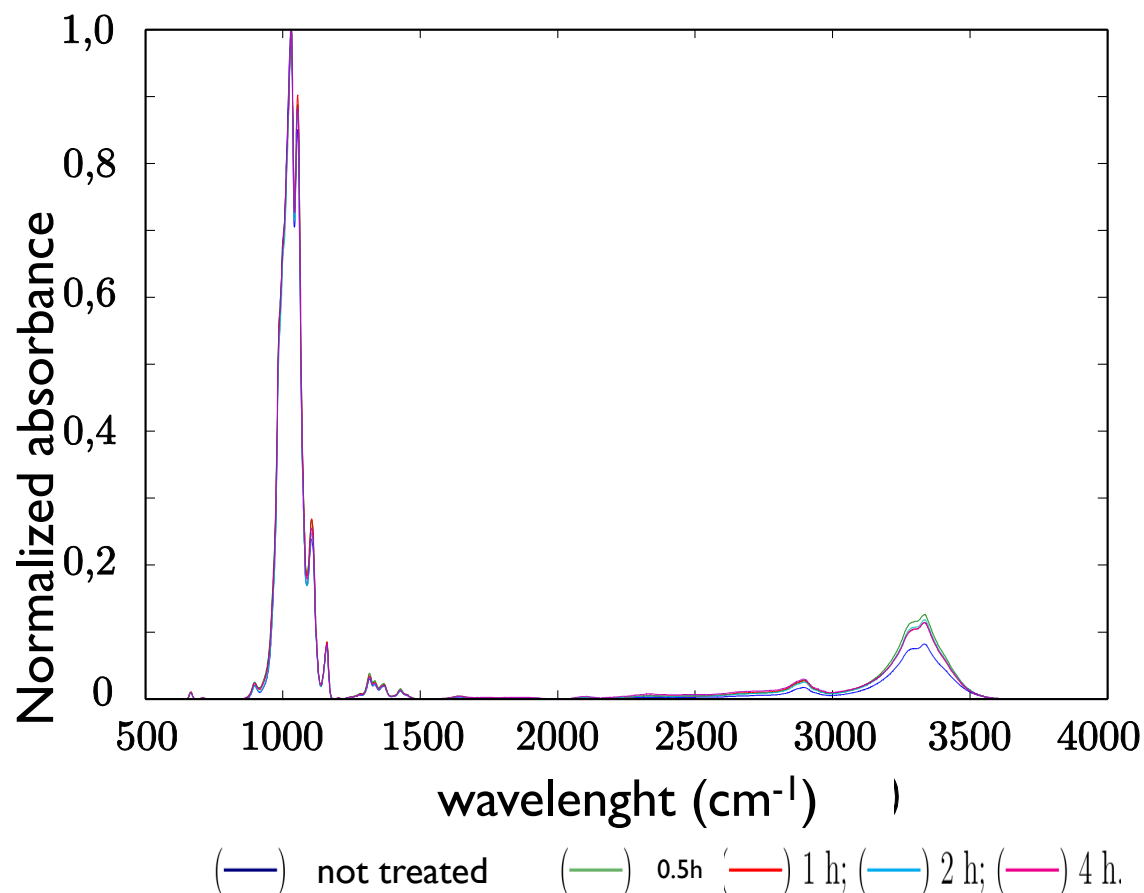
By Jayr Amorim, Carlos Oliveira, Jorge A. Souza-Correa, Marco A. Ridenti
Plasma Process. Polym. 2013, DOI: 10.1002/ppap.201200158



Diffuse Reflectance Fourier Transform Infrared Spectrometry (DRIFT)

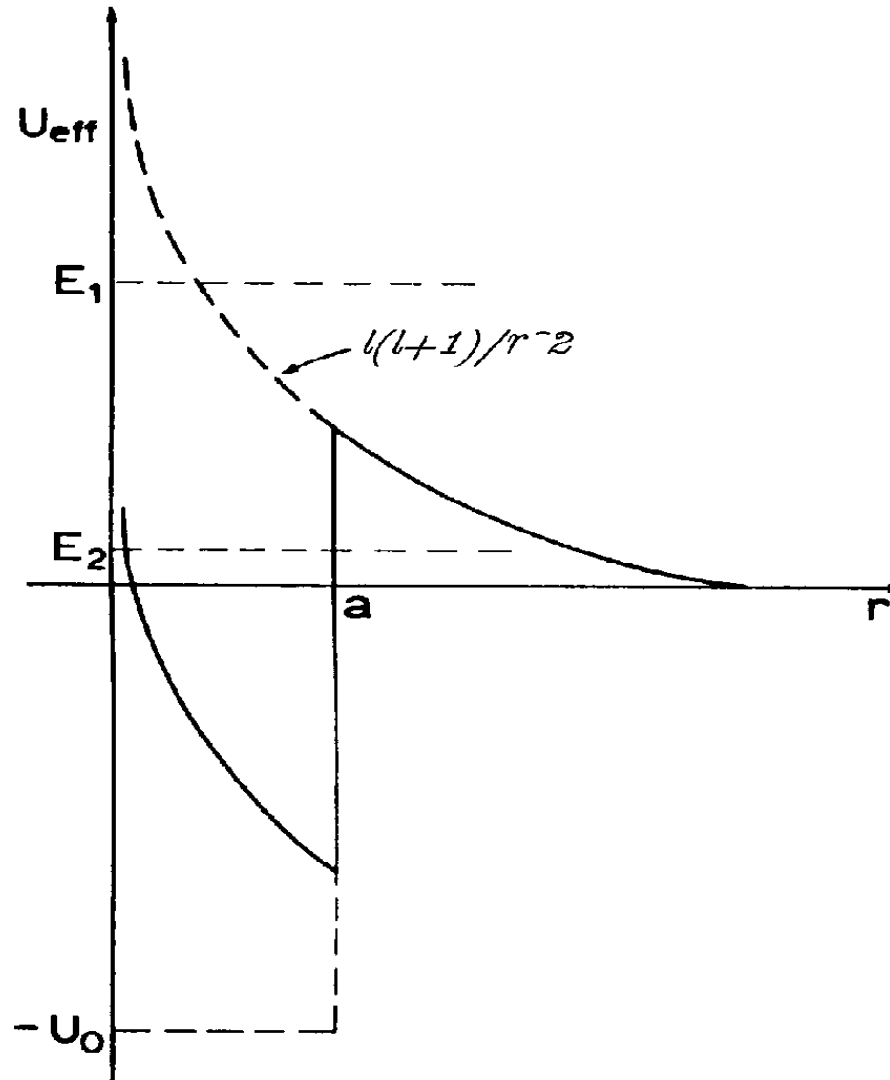


➔ No modification was observed in the spectra after plasma treatment on cellulose



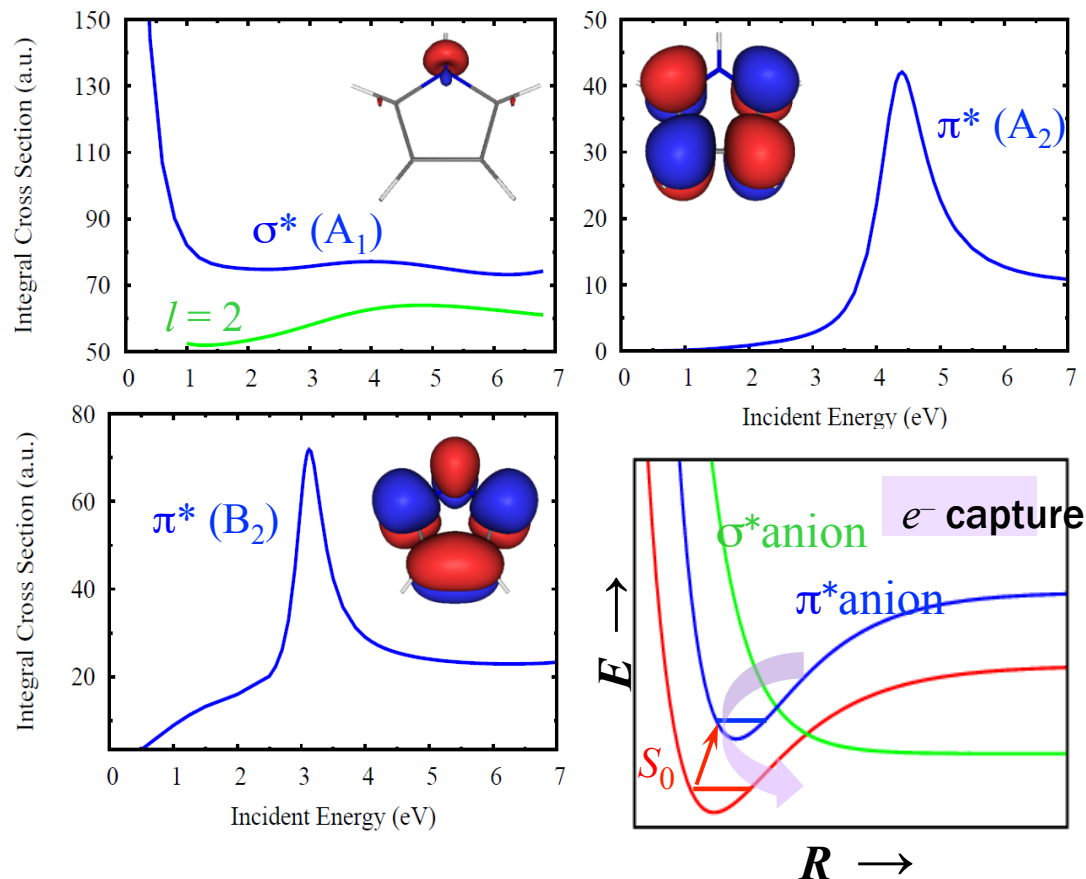
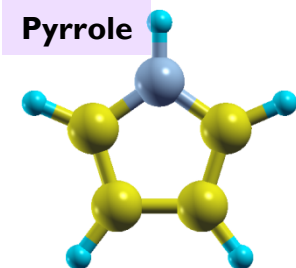
By Jayr Amorim, Carlos Oliveira, Jorge A. Souza-Correa, Marco A. Ridenti
Plasma Process. Polym. 2013, DOI: 10.1002/ppap.201200158

Shape resonances are related to angular momentum traps



Low energy elastic electron scattering from pyrrole

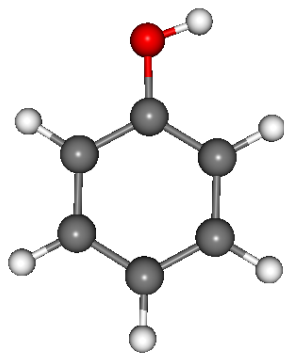
- There are π^* (ring) and σ^* (N-H) shape resonances in pyrrole. Nice prototype!



de Oliveira EM, Lima MAP, Bettega MHF, Sanchez SD, da Costa RF, and Varella MTD, J. Chem. Phys. **132**, 204301 (2010)

Lignin Subunits

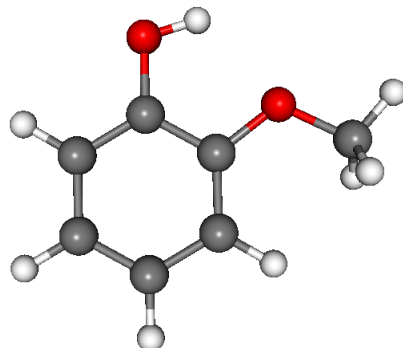
Phenol



MetOH



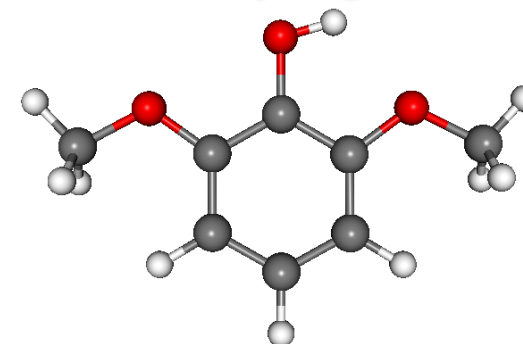
Guaiacol



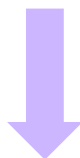
MetOH



Syringol



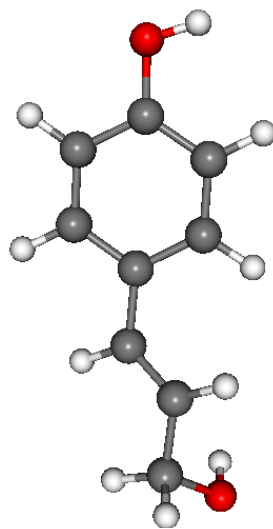
PropenylOH



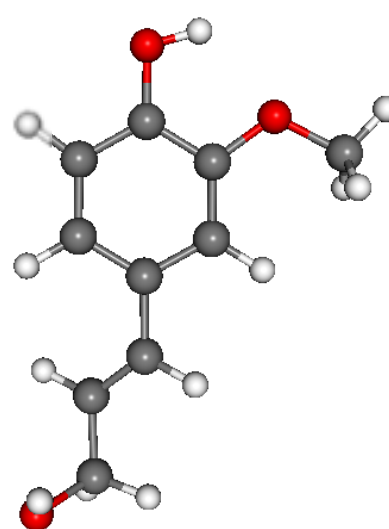
PropenylOH



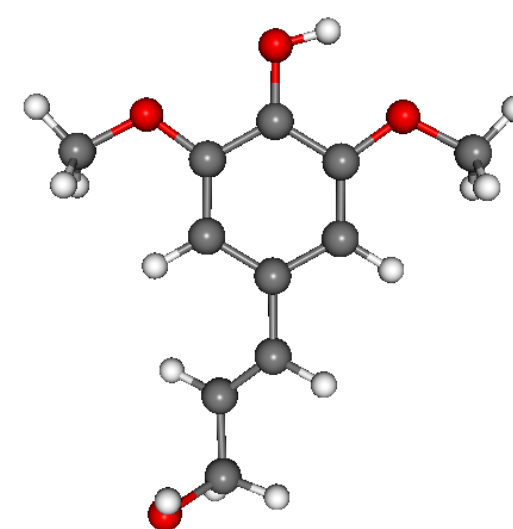
PropenylOH



p-coumaryl alcohol



coniferyl alcohol

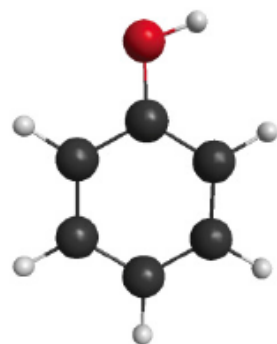


sinapyl alcohol

RAPID COMMUNICATIONS

Shape resonance spectra of lignin subunits

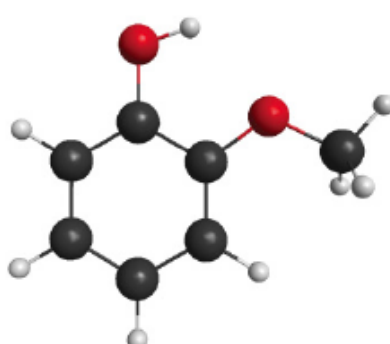
PHYSICAL REVIEW A 86, 020701(R) (2012)



phenol



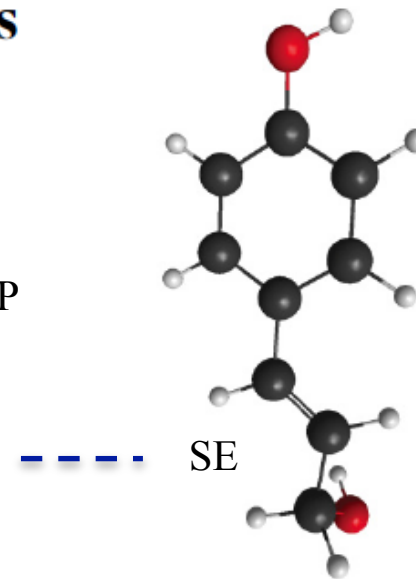
SEP
SE



guaiacol

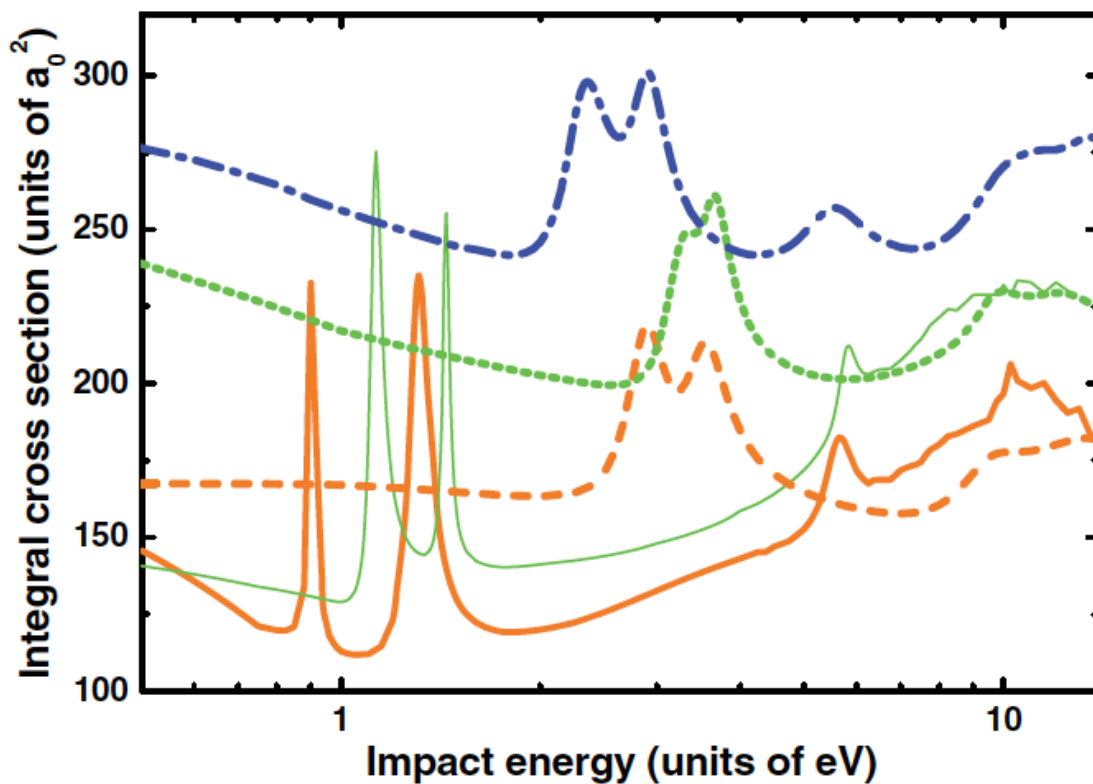
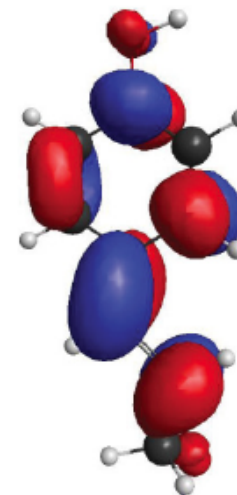


SEP
SE

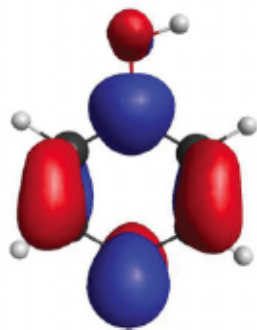


SE

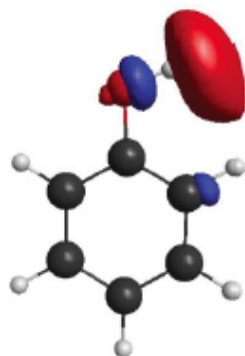
p-coumaryl alcohol
p-Cu (LUMO)



Lots of low-energy resonances!

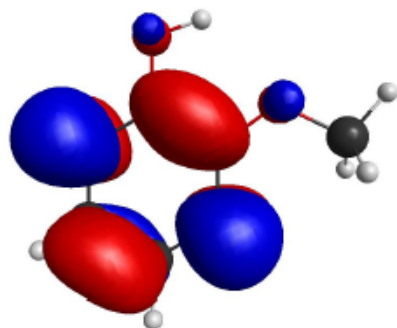


π^* (LUMO+1)

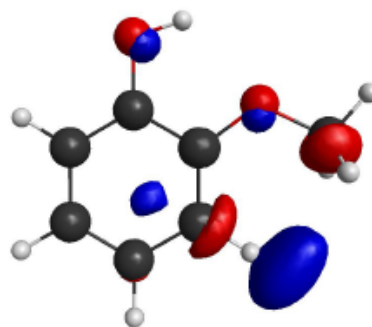


σ^* (LUMO+2)

Phenol: Calculations, ET spectra and DEA data indicate H elimination from π^*/σ^* coupling.

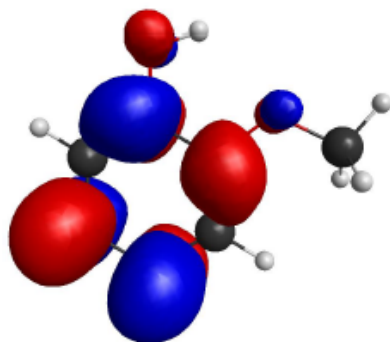


π^* (LUMO)

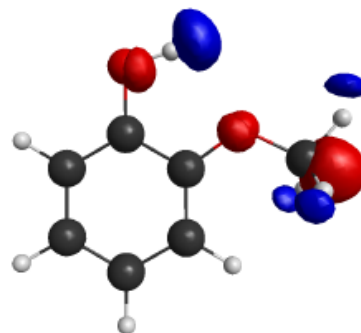


σ^* (LUMO+2)

Guaiacol: Methoxilation is expected to give rise to other dissociation channels. H elimination should be also observed.



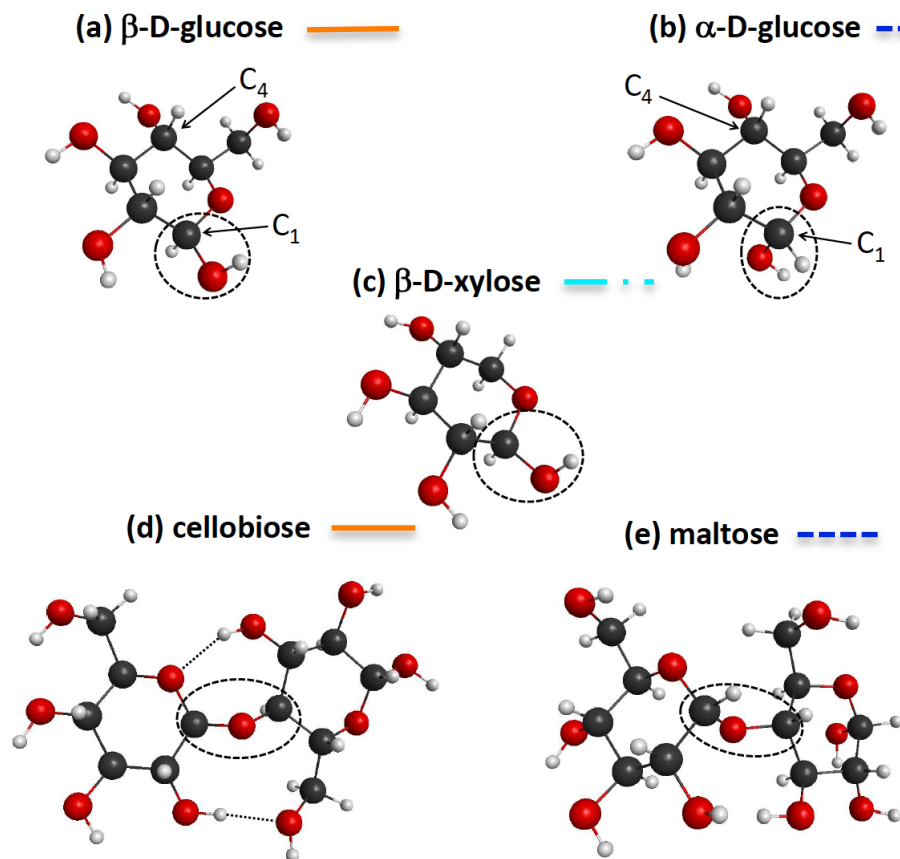
π^* (LUMO+1)



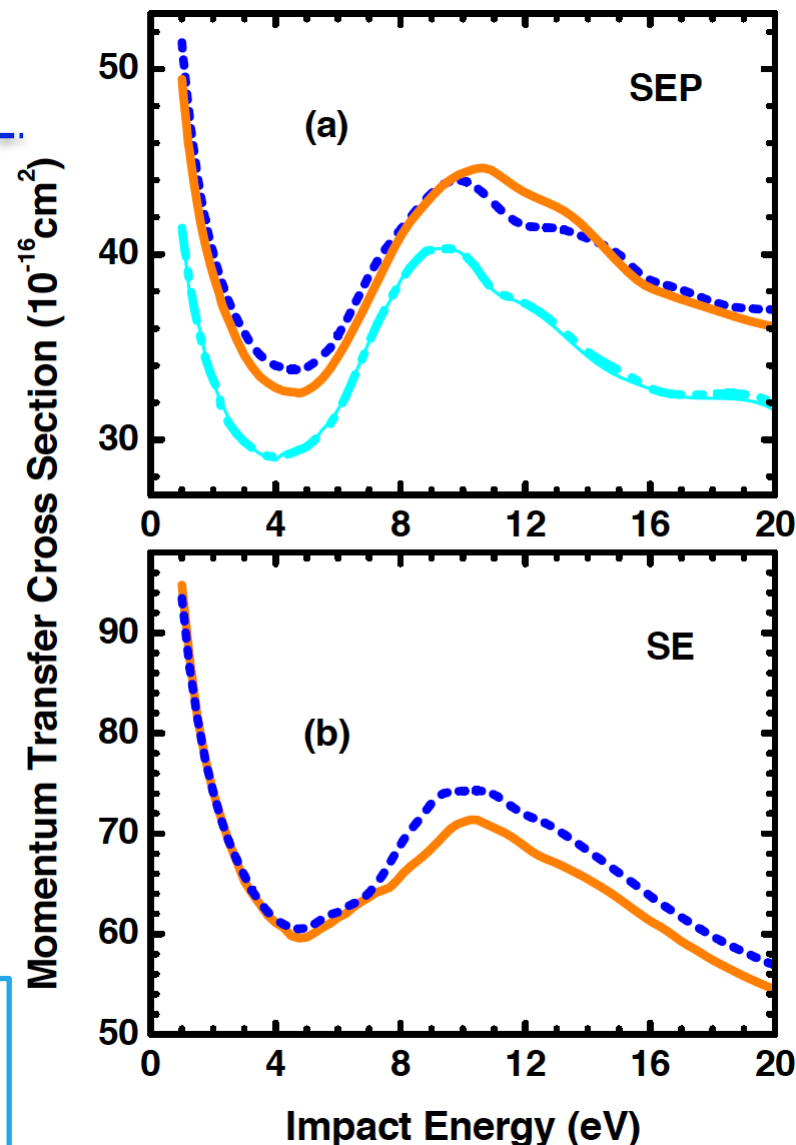
σ^* (LUMO+3)

Low-energy electron scattering by cellulose and Hemicellulose components

Phys. Chem. Chem. Phys. **15**, 1682 (2013).



No low-energy resonances! Is this sufficient to explain why the discharge attacks the lignin and not so much the cellulose and hemicellulose?

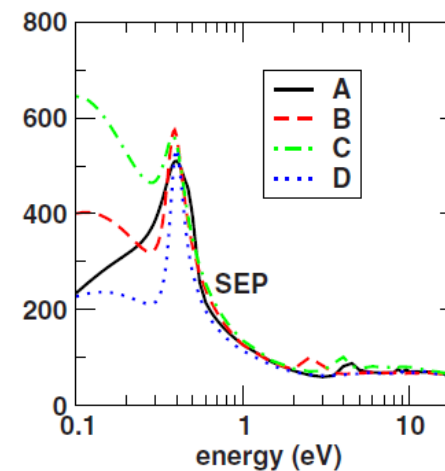
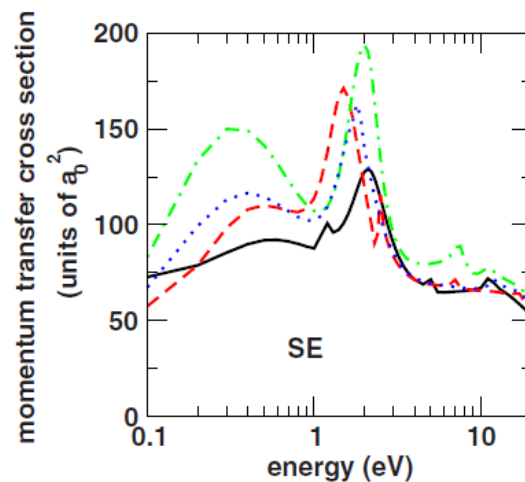
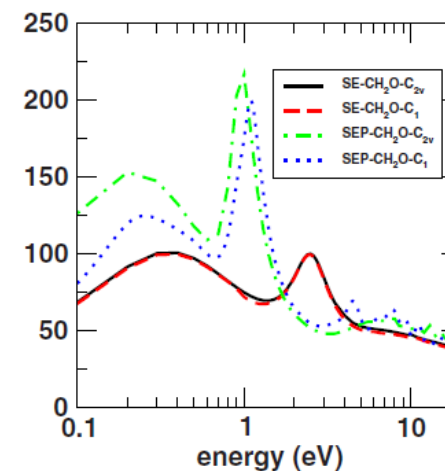
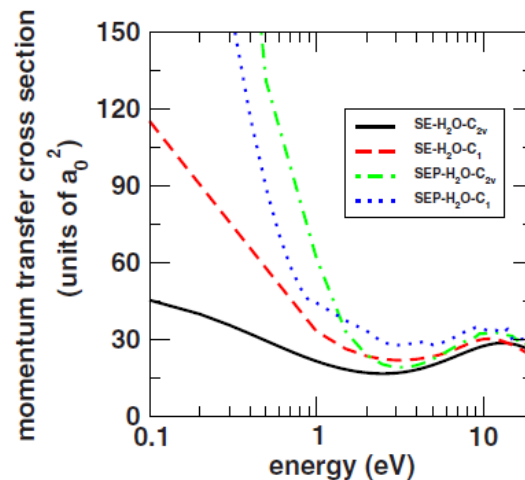
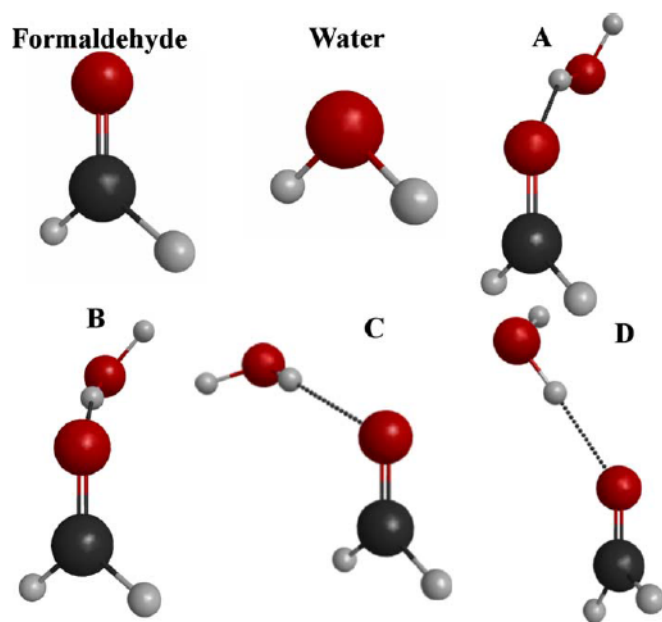


Micro-solvation in elastic scattering

Simple first step towards more realistic situations

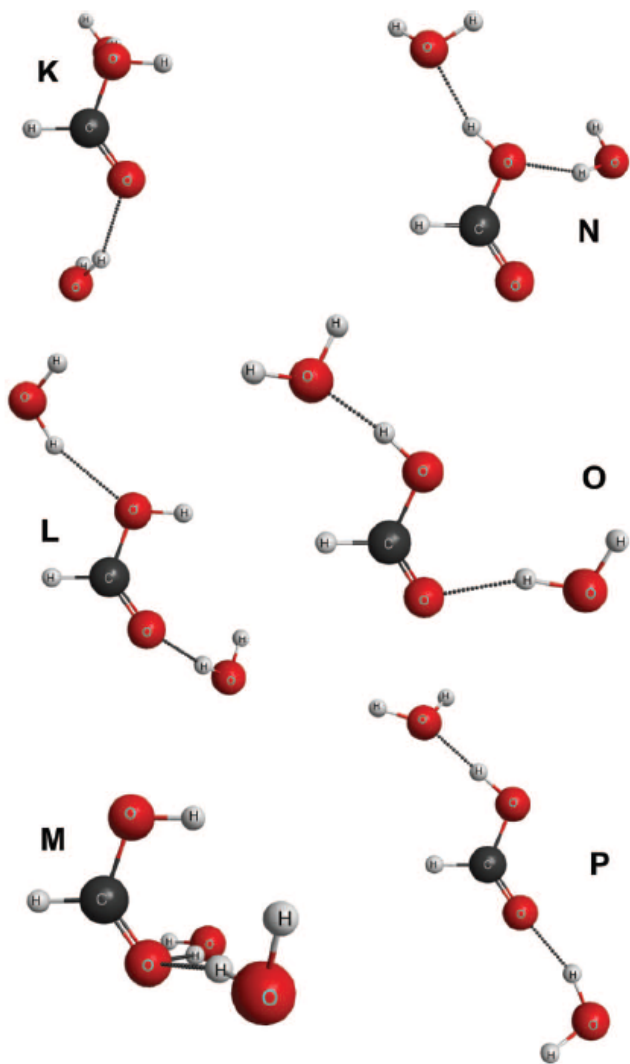
Electron Collisions with the CH₂O-H₂O complex

PHYSICAL REVIEW A 80, 062710 (2009)

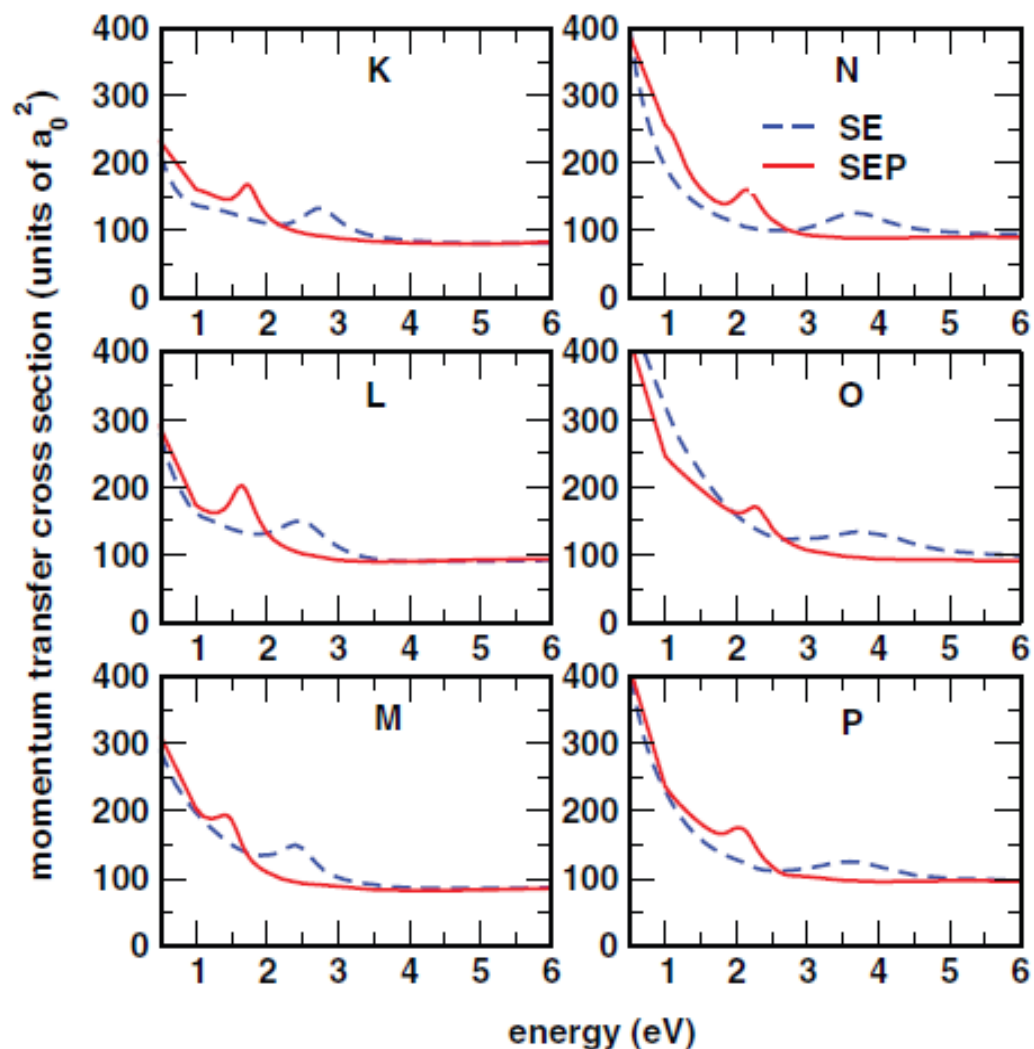


Electron collisions with the HCOOH...(H₂O)_n complexes (n=1, 2) in liquid phase: The influence of microsolvation on the π^* resonance of formic acid

THE JOURNAL OF CHEMICAL PHYSICS 138, 174307 (2013)



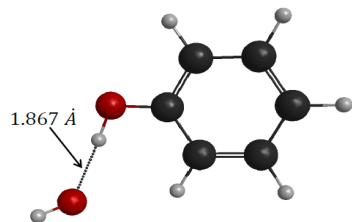
π^* shape resonance for HCOOH at around 1.9 eV.



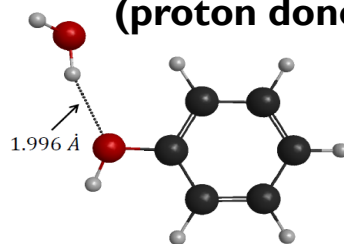
Electron Collisions with Phenol...H₂O

E. M. de Oliveira, T. C. Freitas, K. Coutinho, M. T. do N. Varella, S. Canuto, M. A. P. Lima and M.H.F Bettega, The Journal of Chemical Physics 141, 051105 (2014)

(proton acceptor)



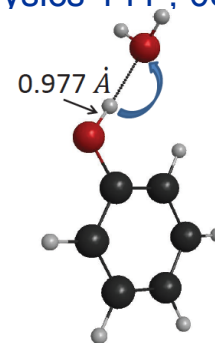
(proton donor)



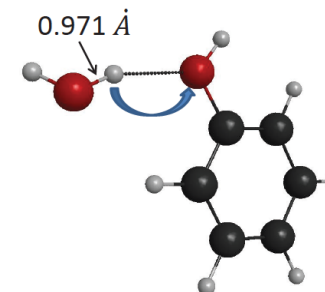
We have studied the microsolvation of Phenol using 4 complexes.

- In Complex A, the water molecule is a proton acceptor.
- In the Complex B, the water is a proton donor.
- Complexes C and D have both situations (one water molecule as acceptor and the other as proton donor).

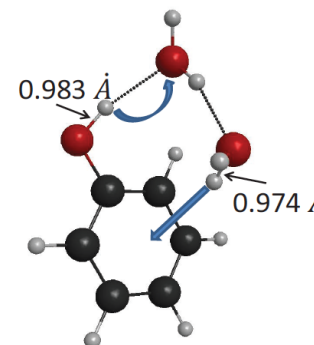
In real situations the resonances may change positions due to an overall donor or acceptor effect!



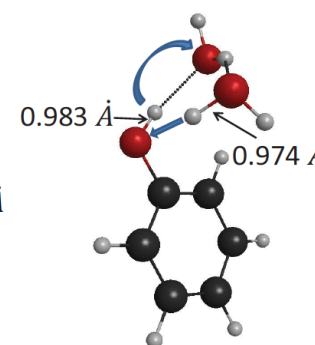
CoA



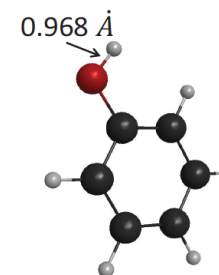
CoB



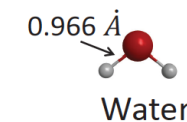
CoC



CoD

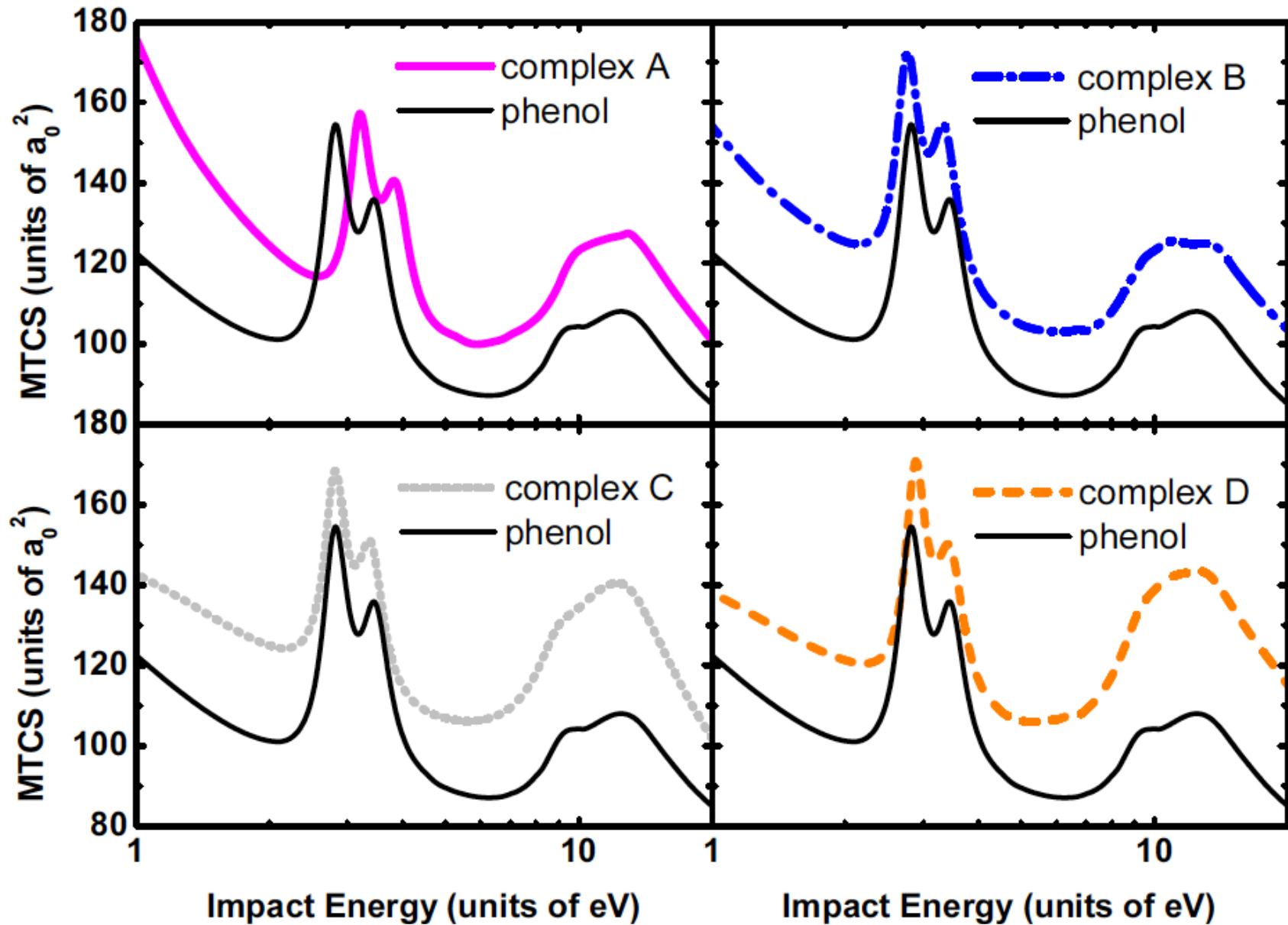


Ph



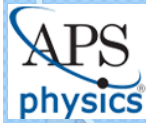
Water

Electron Collisions with Phenol...(H_2O)_n: n=1,2



How useful are these calculations to a modeler?

68th GEC
9th ICRP
33rd SPP
12-16 Oct. 15
Honolulu

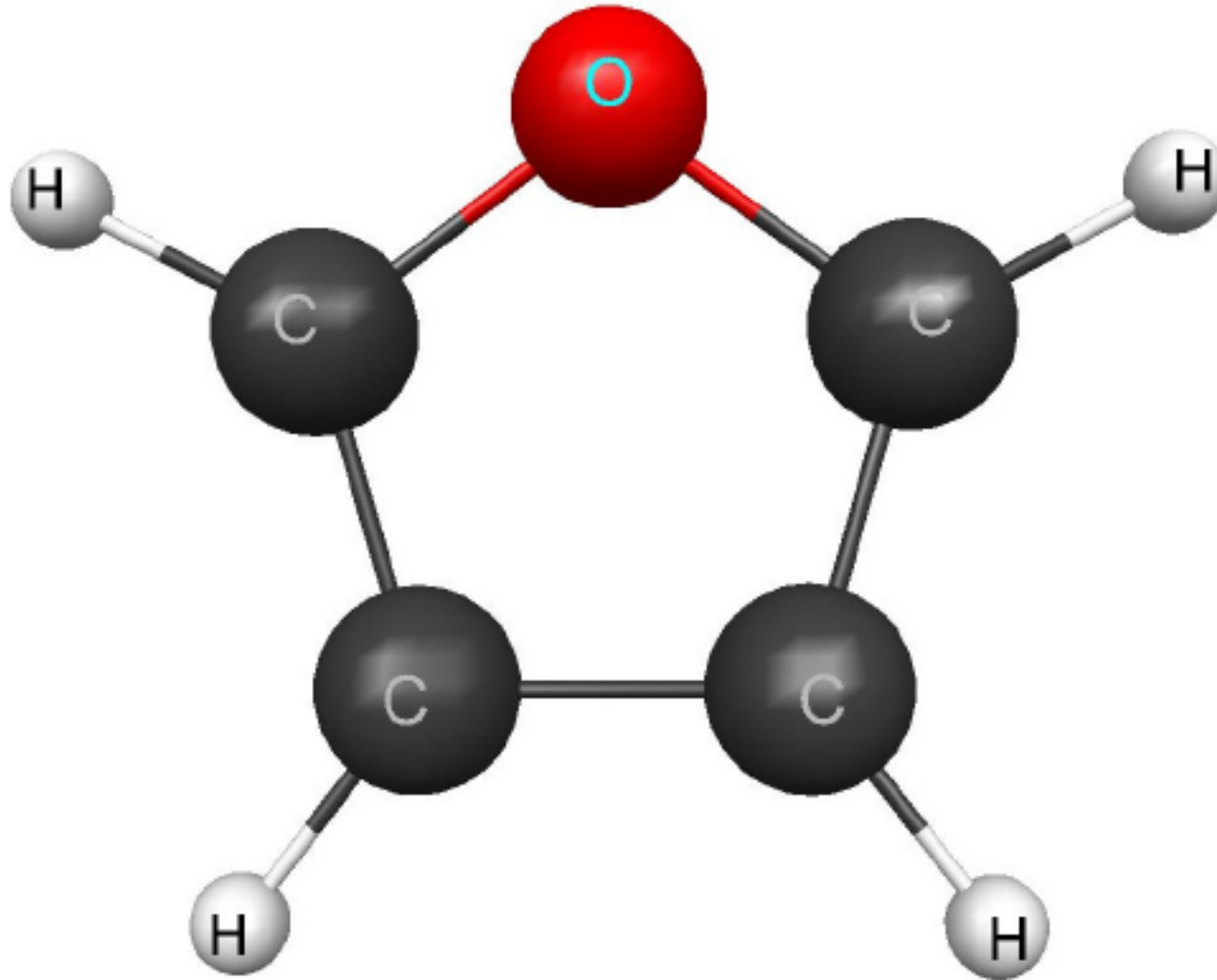


ELECTRONIC EXCITATION



38
MAPLima

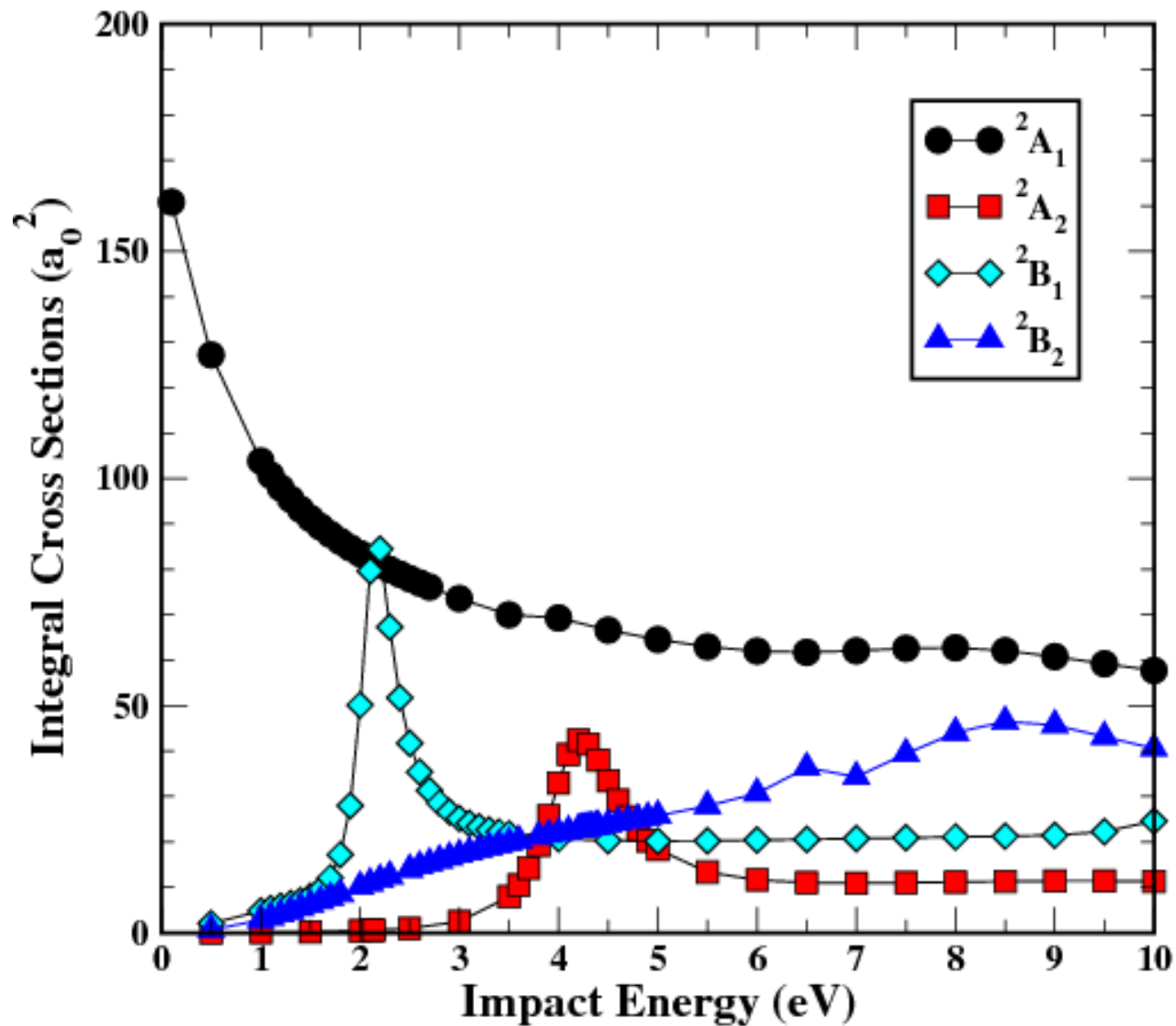
Electronic excitation of furan by electron impact



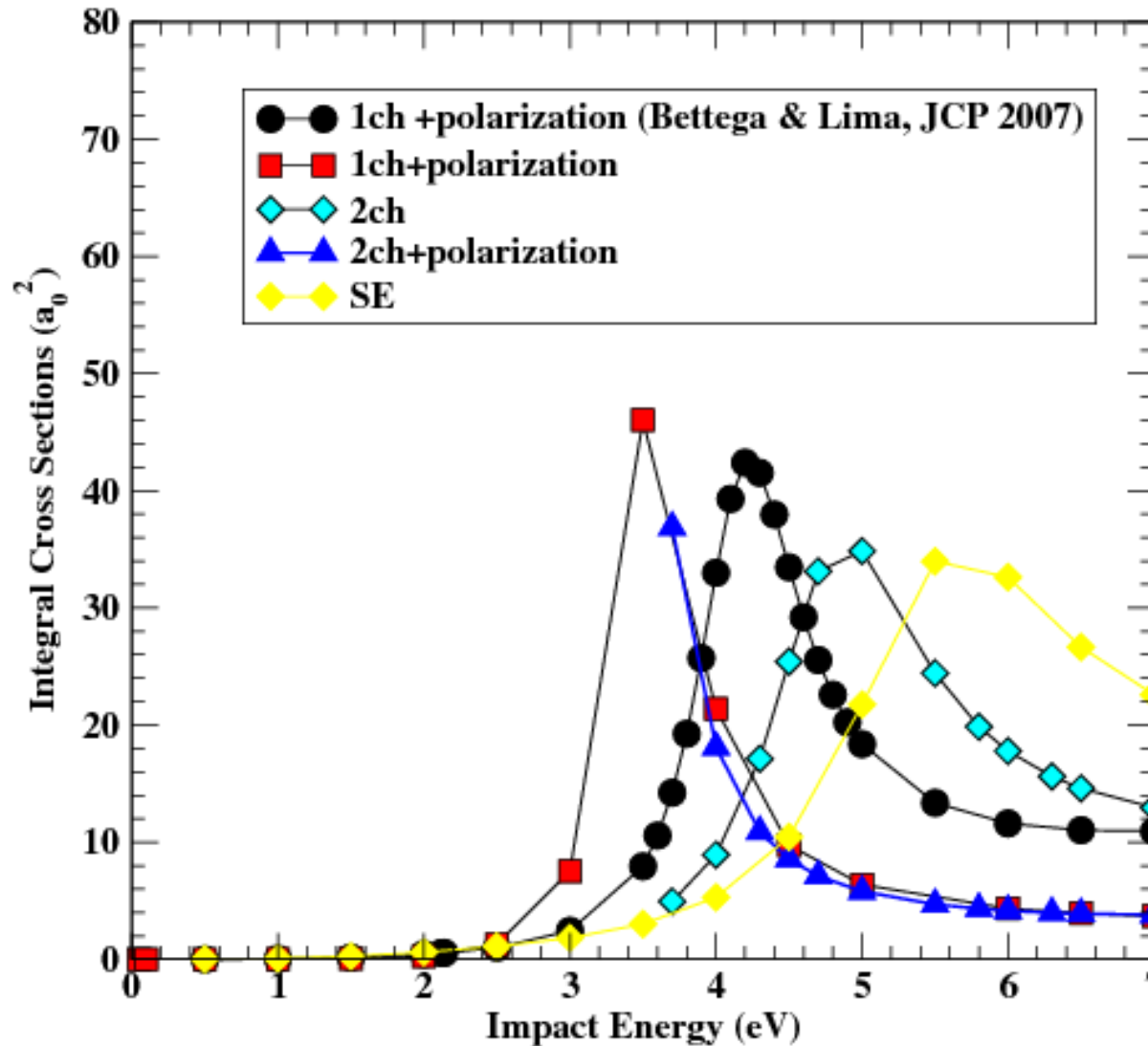
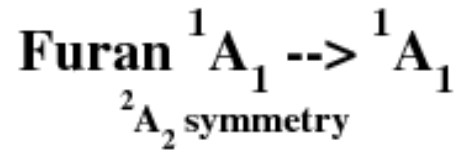
Furan presents two shape resonances at low impact energies

Electron-Furan Scattering

Bettega & Lima, J. Chem. Phys. (2007)

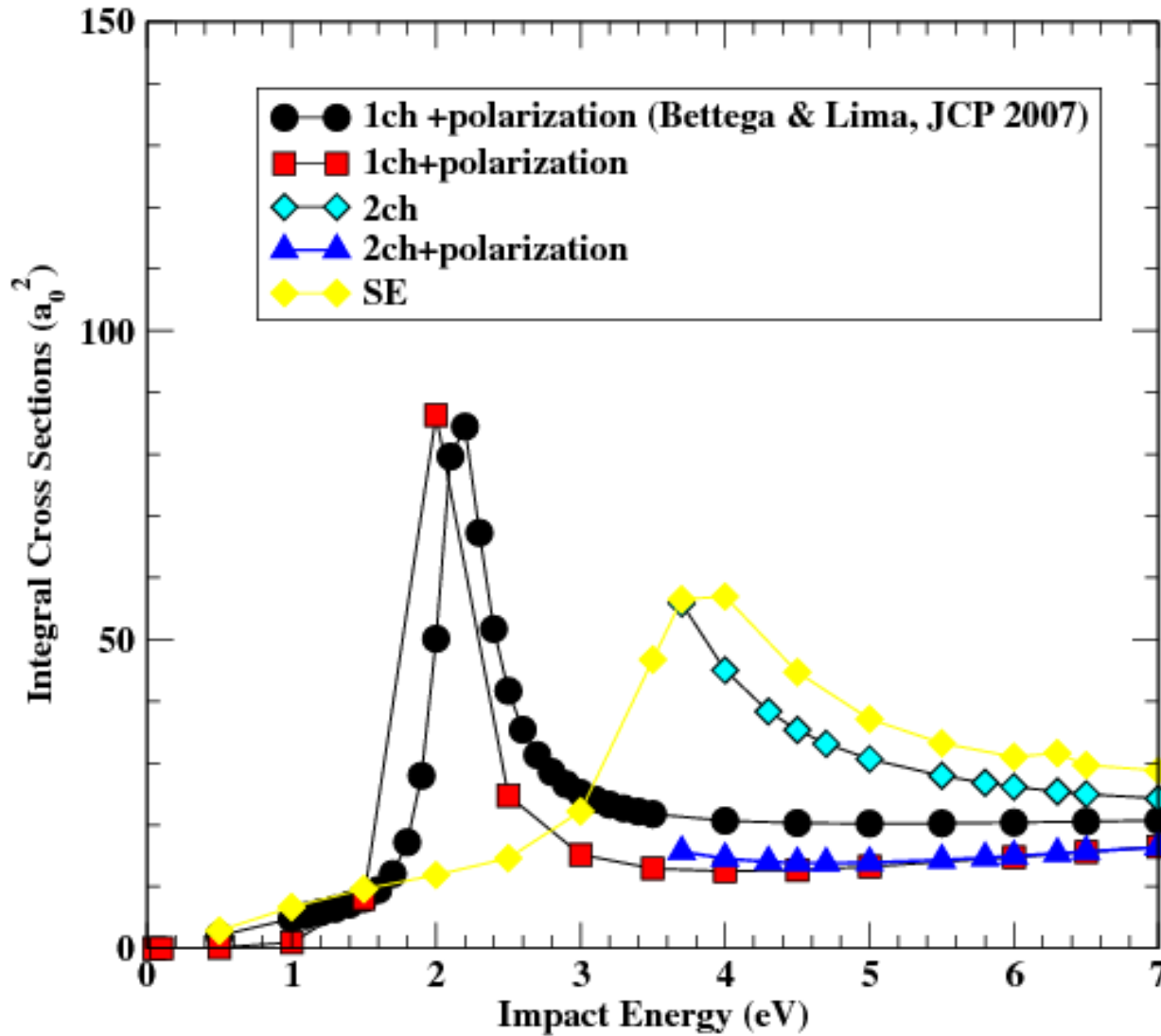
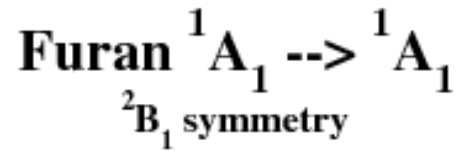


Polarization effects strongly affect the resonance positions



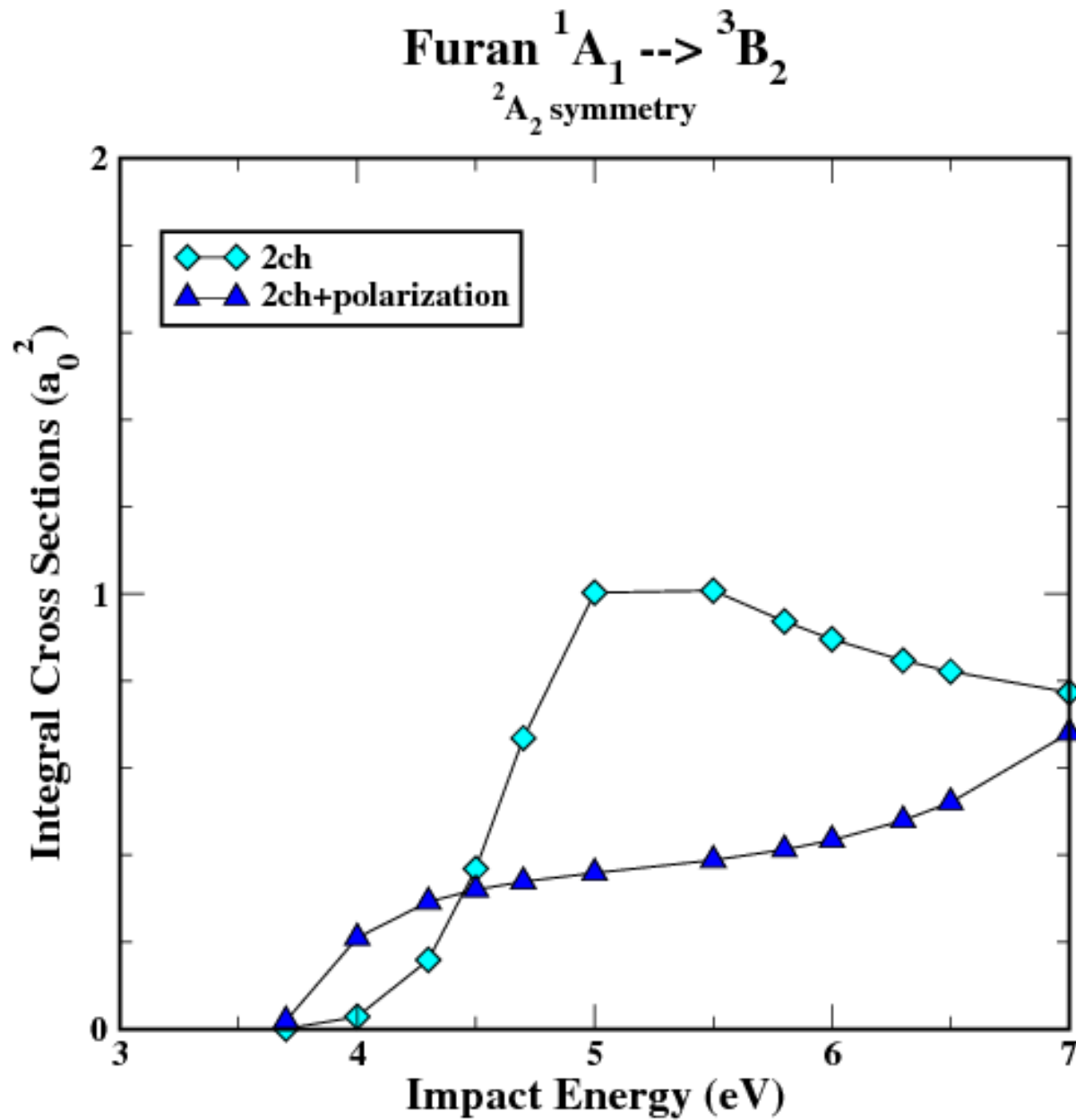
Finding resonance's positions and widths may not be enough!

Polarization effects strongly affect the resonance positions



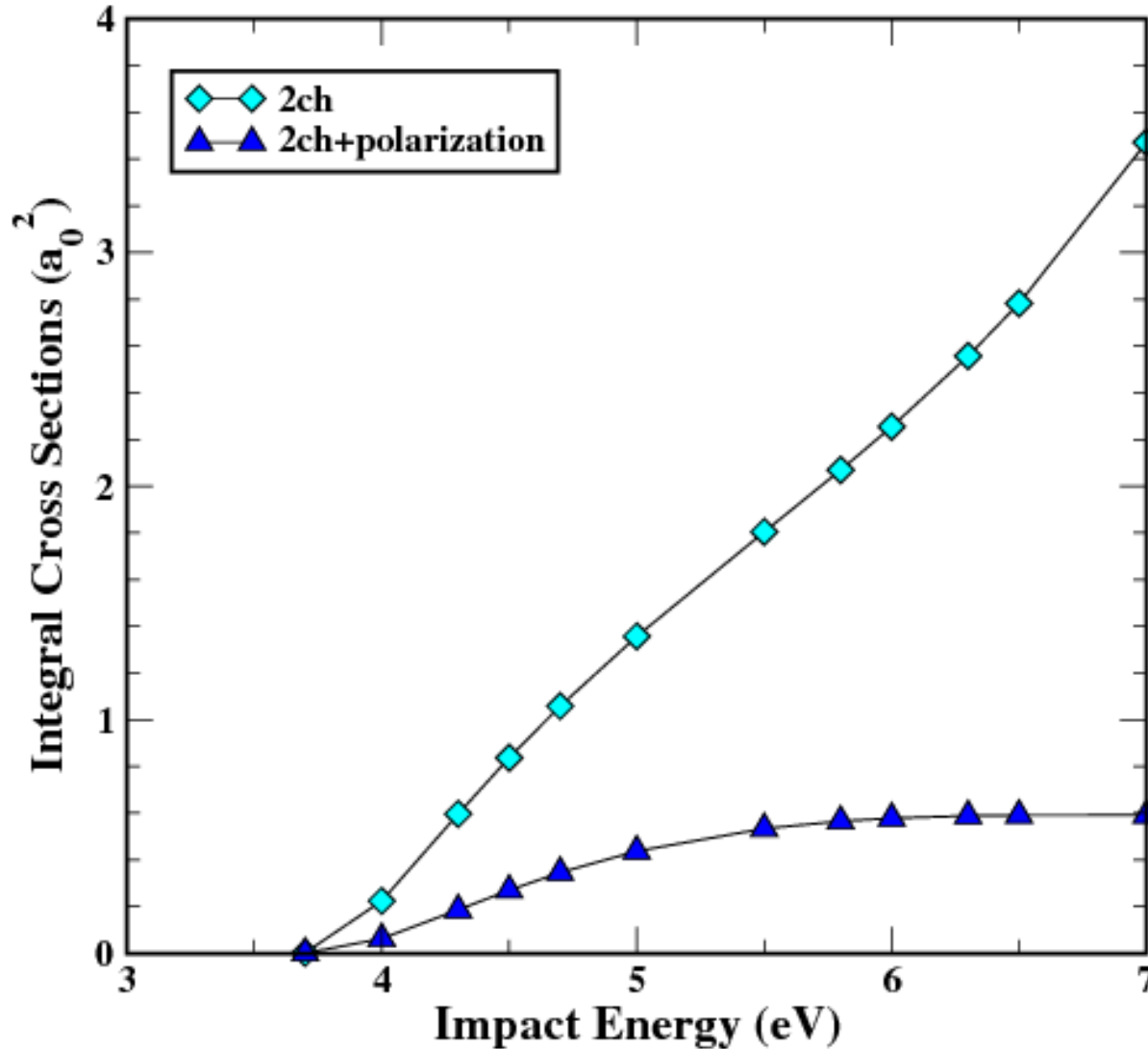
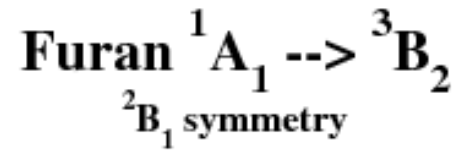
Finding resonance's positions and widths may not be enough!

The resonance positions strongly affect the excitation cross sections



How would that affect a plasma modeling?

The resonance positions strongly affect the excitation cross sections



How would that affect a plasma modeling?

Electronic excitation of Phenol by electron impact

D. B. Jones, G. B. da Silva, R. F. C. Neves, H.V. Duque, L. Chiari, E. M. de Oliveira, M. C.A. Lopes, R. F. da Costa, M.T. do N.Varella, M. H. F. Bettega, M. A. P. Lima, and M.J. Brunger, *J. Chem. Phys.* **141**, 074314 (2014). First of a series of papers under the Science without Border Program (CNPq/CAPES).

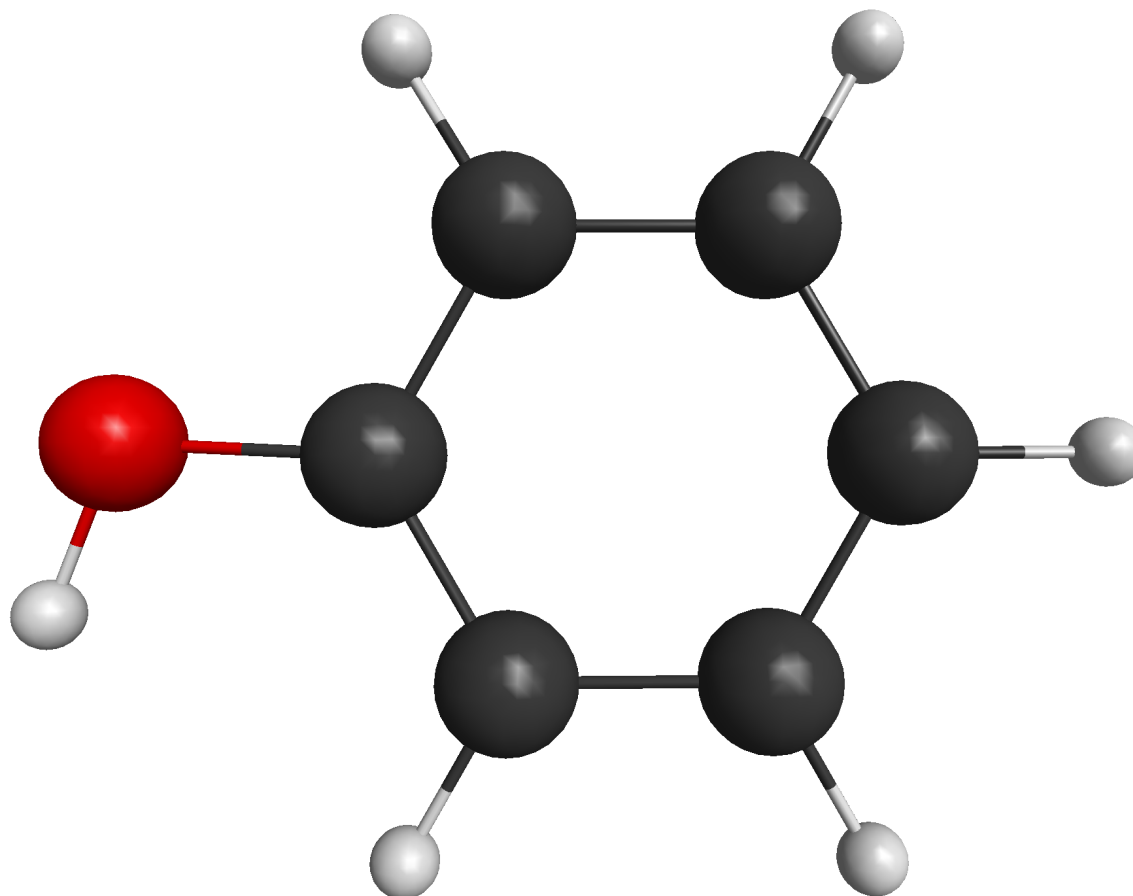


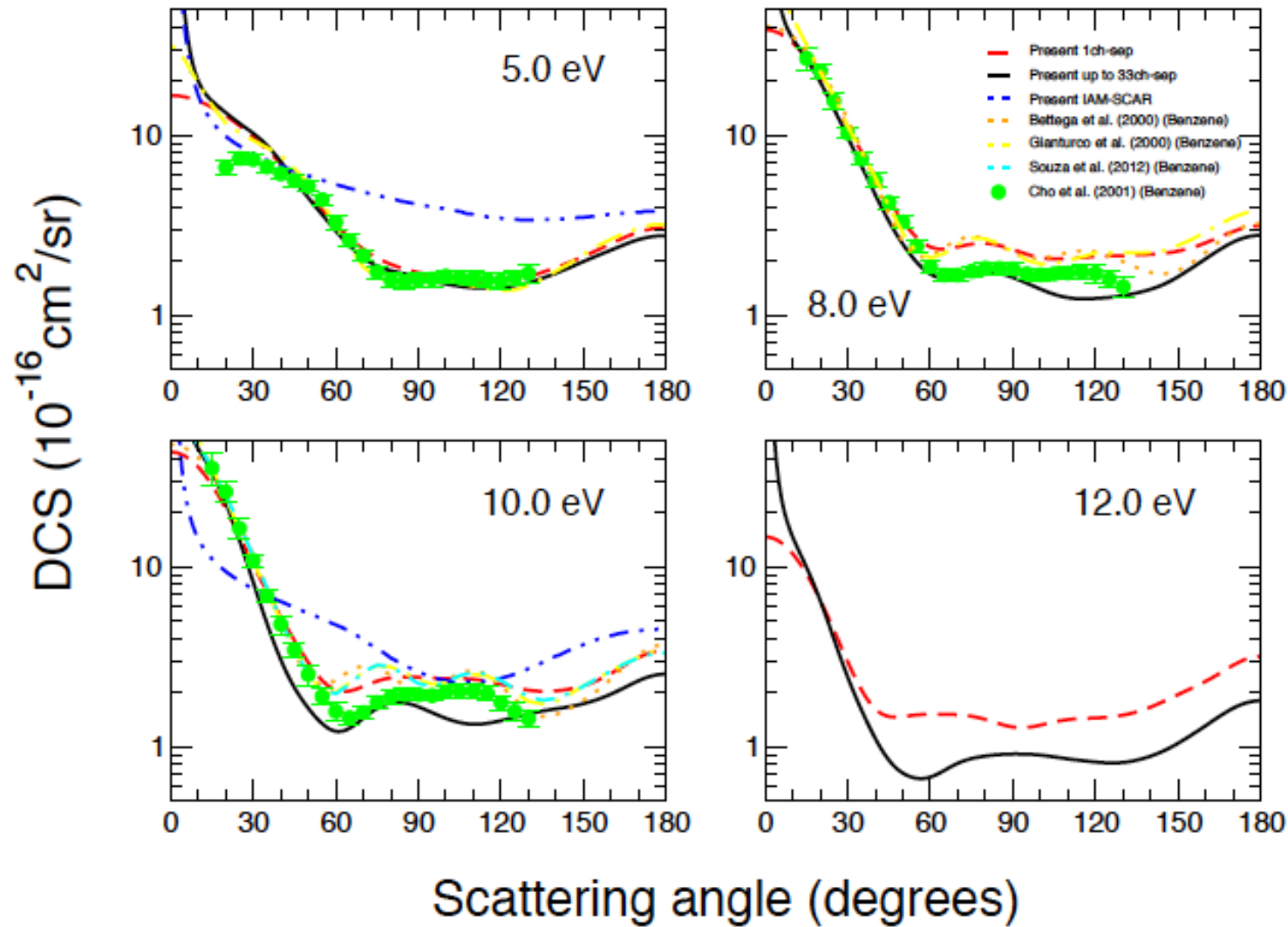
TABLE I. Experimental and calculated excitation energies, assignments, dominant configurations, and optical oscillator strengths (f_0).

Band	Expt. energy (eV)	State	TD-DFT			MOB-SCI		Full-SCI	
			Energy (eV)	Dominant excitation(s)	f_0	Energy (eV)	f_0	Energy (eV)	f_0
I	3.4–4.3	³ A'	3.71	3a'' → 5a''; 4a'' → 6a''	0	3.57	0	3.29	0
		³ A'	4.10	4a'' → 5a''	0	4.73	0	4.49	0
II	4.3–5.4	³ A'	4.53	3a'' → 5a''; 4a'' → 6a''	0	4.90	0	4.78	0
		¹ A'	4.99	3a'' → 6a''; 4a'' → 5a''	0.0312	6.09	0.0248	5.82	0.0381
		³ A''	5.06	4a'' → 22a'	0	6.16	0	5.94	0
		¹ A''	5.13	4a'' → 22a'	0.0001	6.21	0.0001	6.06	0.0001
		³ A'	5.30	3a'' → 6a''	0	6.03	0	5.73	0
III	5.4–6.3	³ A''	5.53	4a'' → 23a'	0	6.78	0	6.53	0
		¹ A''	5.57	4a'' → 23a'	0.0034	6.86	0.0274	6.68	0.0177
		¹ A'	5.76	3a'' → 5a''; 4a'' → 6a''	0.0328	6.80	0.0031	6.12	0.0025
		³ A''	5.90	3a'' → 22a'; 4a'' → 24a'	0	6.92	0	6.73	0
		¹ A''	5.92	4a'' → 24a'	0				
		³ A''	5.95	3a'' → 22a'; 4a'' → 24a'	0				
		¹ A''	5.98	3a'' → 22a'	0.0021	6.99	0	6.86	0.0020
		³ A''	6.27	4a'' → 25a'	0				
		IV	6.3–7.3	¹ A''	6.31	4a'' → 25a'	0.0115		
³ A''	6.32			3a'' → 23a'	0				
¹ A''	6.35			3a'' → 23a'	0.0010				
³ A''	6.52			4a'' → 26a'	0				
¹ A''	6.54			4a'' → 26a'	0				
³ A''	6.63			3a'' → 24a'	0				
¹ A'	6.66			3a'' → 6a''	0.3744				
¹ A''	6.66			3a'' → 24a'	0.0202				
¹ A'	6.71			3a'' → 5a''; 4a'' → 6a''	0.5827				
³ A''	6.84			4a'' → 27a'; 4a'' → 28a'	0				
³ A'	6.85			2a'' → 5a''	0				
³ A'	6.93			4a'' → 7a''	0				
¹ A''	6.93			4a'' → 27a'; 4a'' → 28a'	0.0009				
¹ A'	7.01			4a'' → 7a''	0.0148				
³ A''	7.07			3a'' → 25a'	0				
¹ A''	7.08	3a'' → 25a'	0						
³ A'	7.11	2a'' → 6a''	0						
³ A''	7.19	4a'' → 27a'; 4a'' → 28a'	0						
¹ A''	7.22	4a'' → 27a'; 4a'' → 28a'	0.0005						
³ A''	7.27	21a' → 5a''	0						
³ A''	7.29	3a'' → 26a'	0						
V	7.3–8.6	¹ A''	7.32	3a'' → 26a'	0.0002				
		¹ A''	7.57	21a' → 5a''	0.0043				
		³ A''	7.58	4a'' → 29a'	0				
		³ A''	7.59	3a'' → 27a'; 3a'' → 28a'	0				

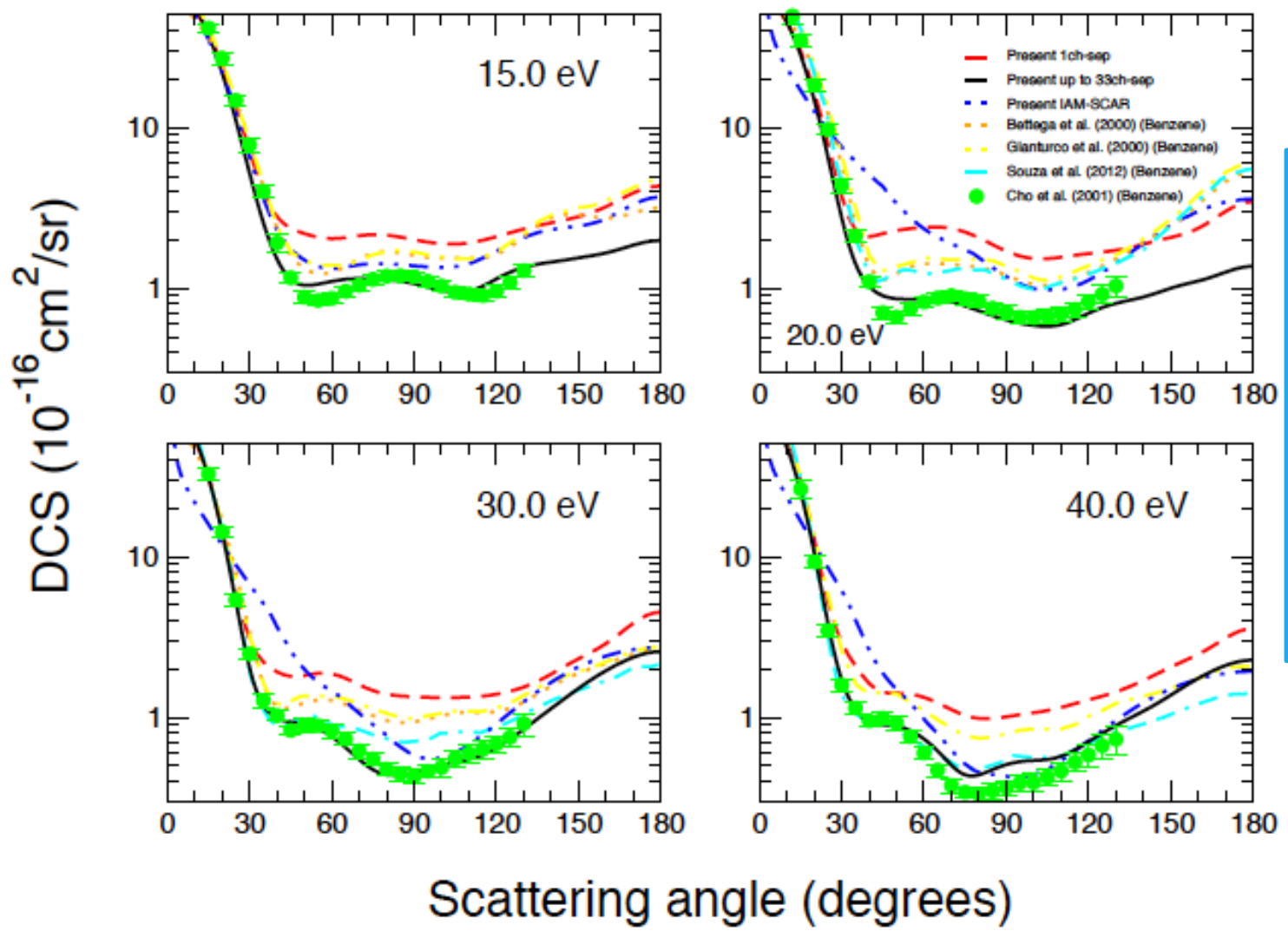
No state-by-state resolution. Our experimental resolution is by bands of electronic states

Our scattering calculations have 5 singlets and 7 triplets below 7eV in good agreement with the full single configuration interaction. We also included 20 additional pseudo states as possible open channels (a total of 33 channels)

Multichannel coupling on electron-Phenol scattering: Effects on the Elastic channel

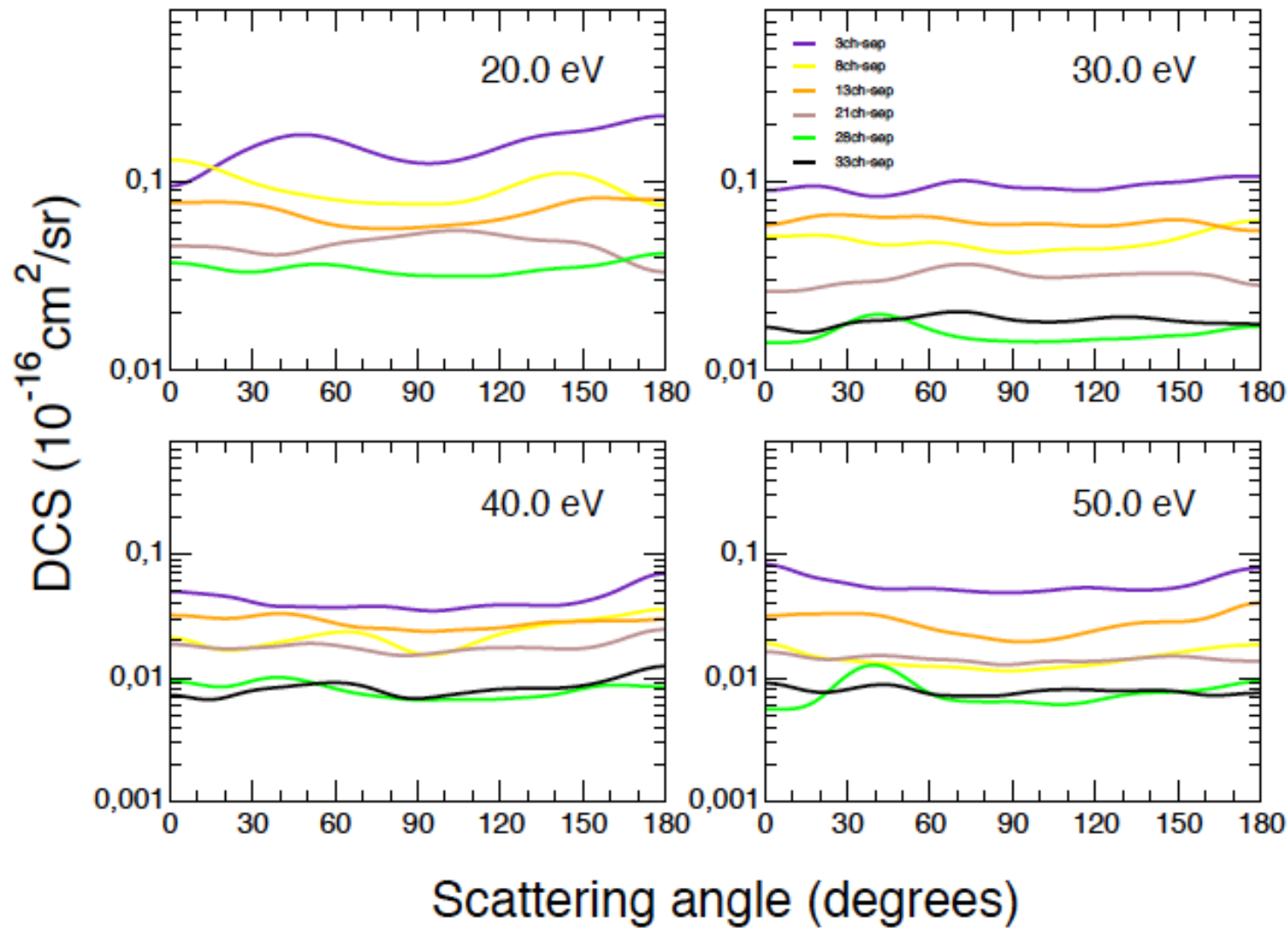


Multichannel coupling on electron-Phenol scattering: Effects on the Elastic channel



Flux competition is a important effect. As we open more channels the flux to a particular state decreases.

Multichannel coupling on electron-Phenol scattering: Effects on the first triplet state channel

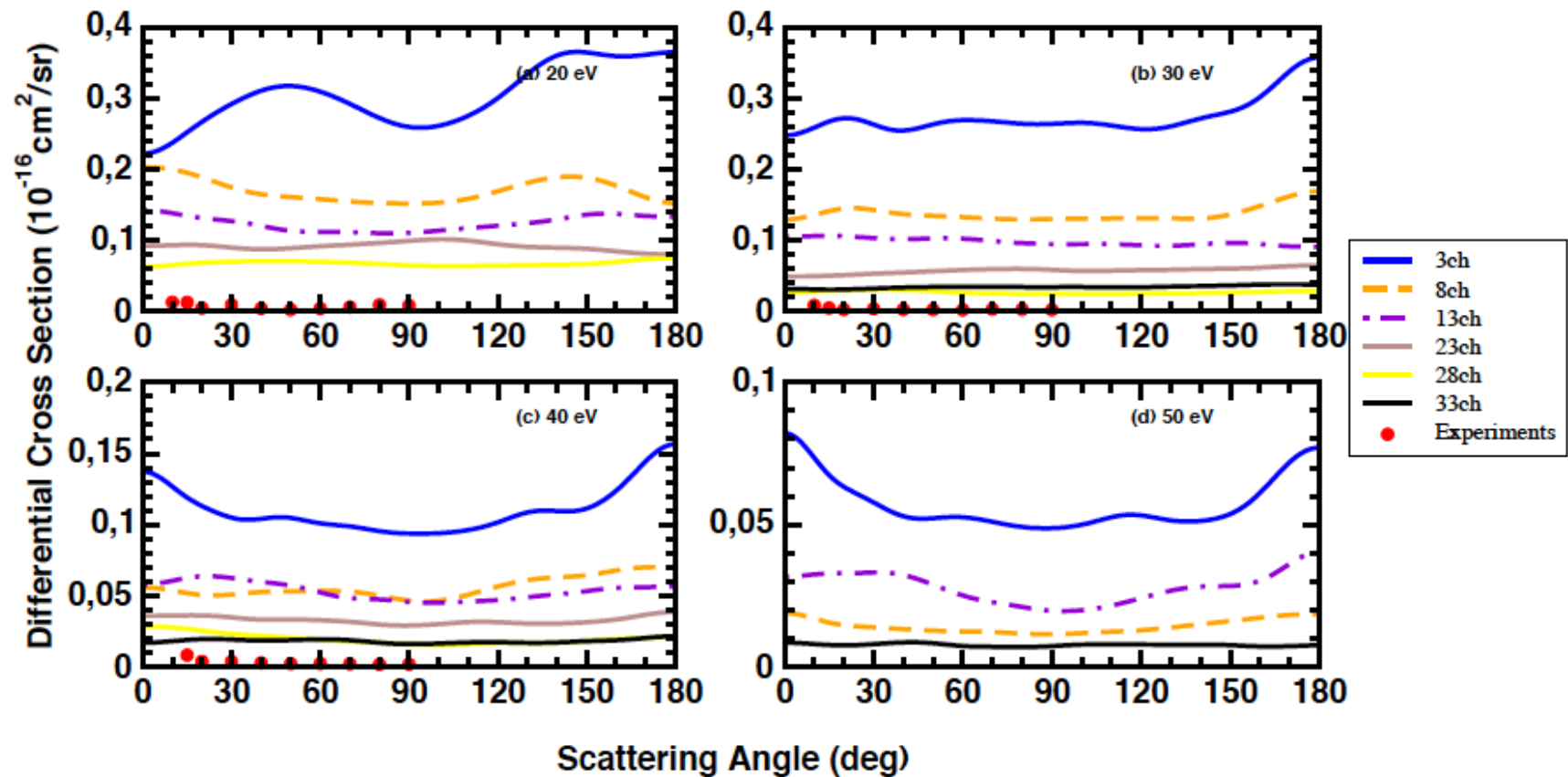


Flux competition is an important effect. As we open more channels the flux to a particular state decreases.

It reminds a classical picture of a river blocked by gates. As you open more gates the flux through all of them decreases.

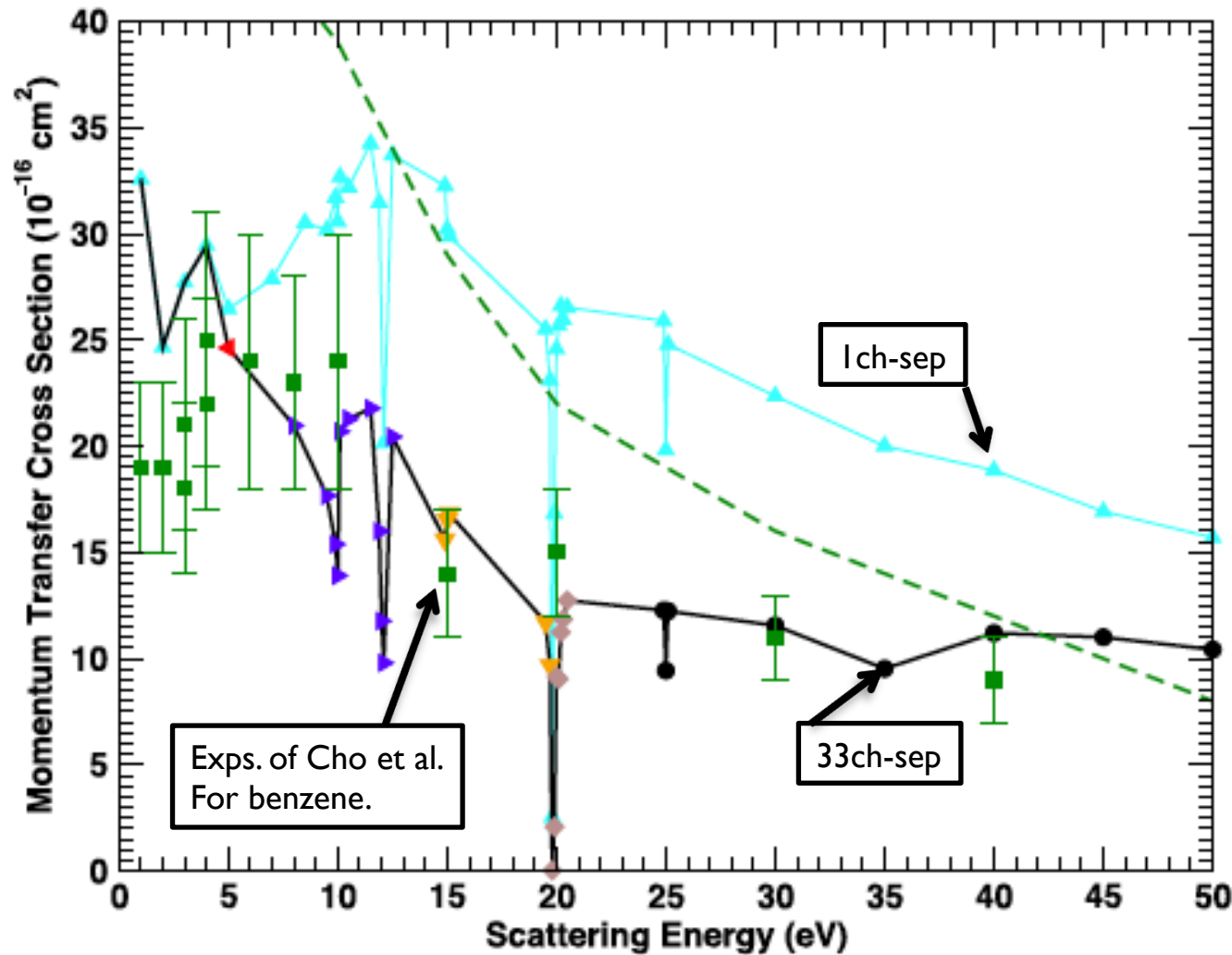
R. F. C. Neves, D. B. Jones, M. C.A. Lopes, K. L. Nixon, G. B. Da Silva, H.V. Duque, E. M. de Oliveira, R. F. da Costa, M.T. do N.Varella, M. H. F. Bettega, M.A. P. Lima, K. Ratnavelu, G. García, and M. J. Brunger, *J. Chem. Phys.* **142**, 104305 (2015).

Phenol: electronic excitation of Band I



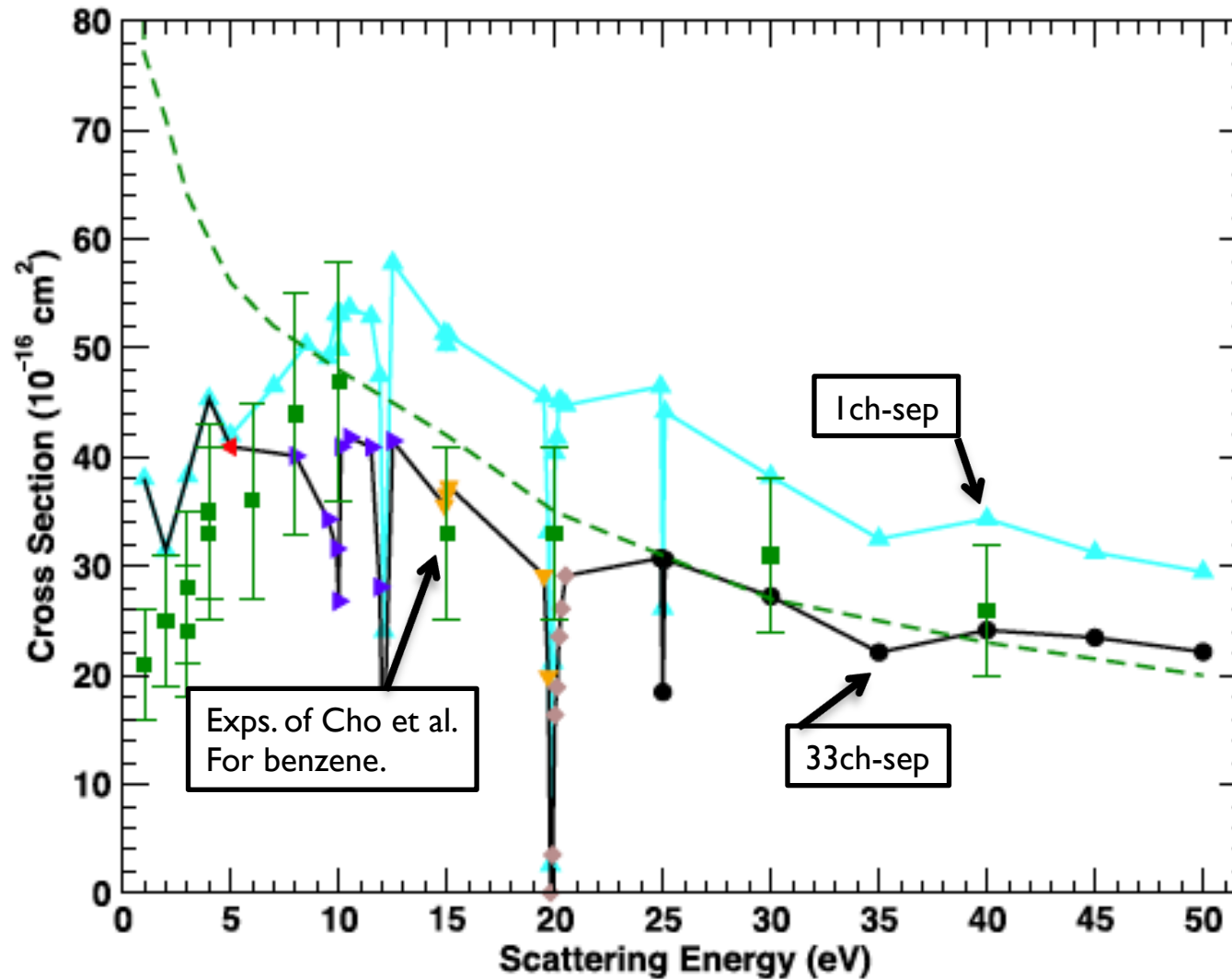
Still a factor of 3-4 from experiments. How would that affect modeling?

Multichannel effects on the elastic momentum transfer cross sections for electron-phenol scattering



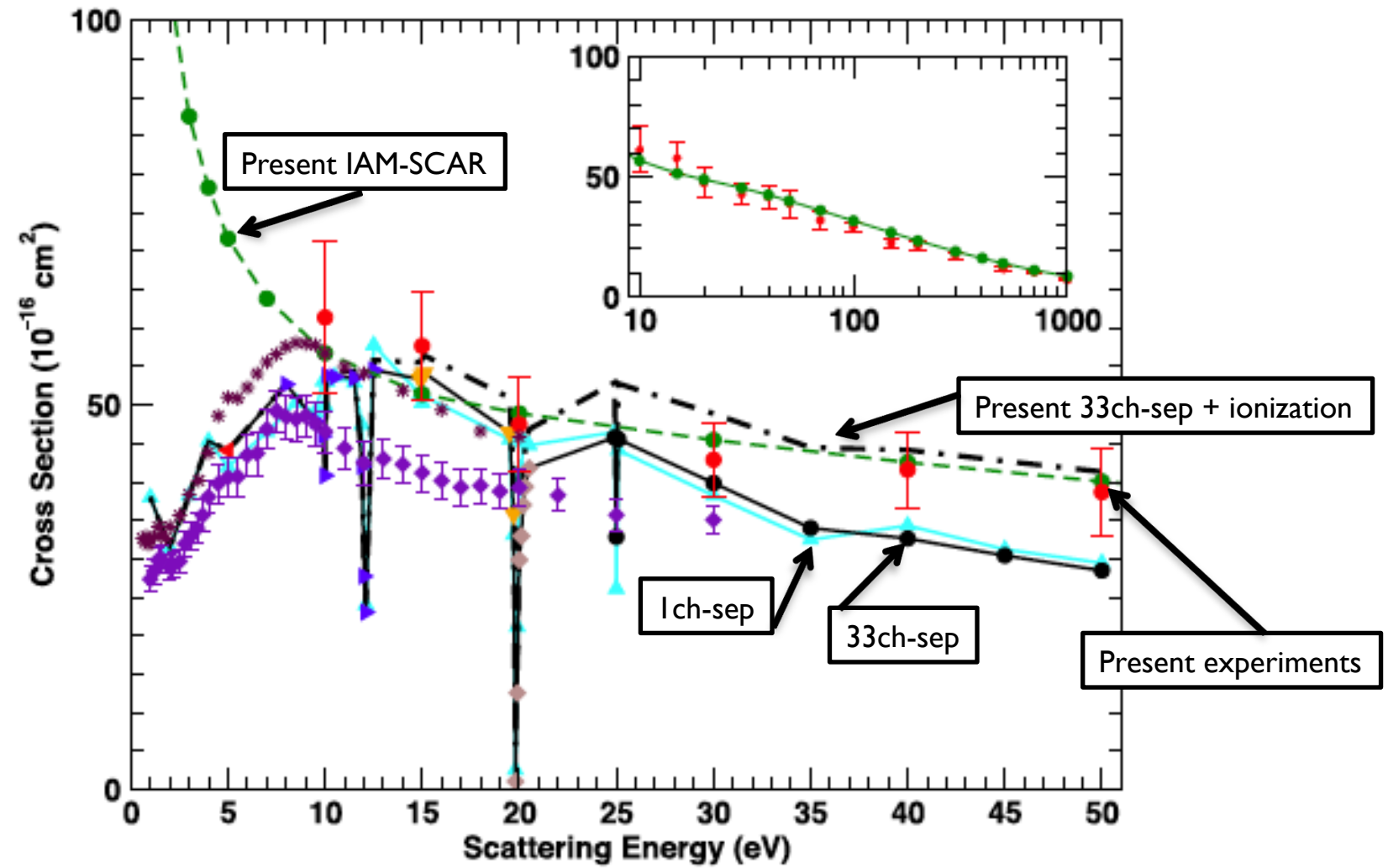
How this big change, caused by multichannel effects, in the MTCS would affect modeling?

Multichannel effects on the elastic **integral cross sections** for electron-phenol scattering



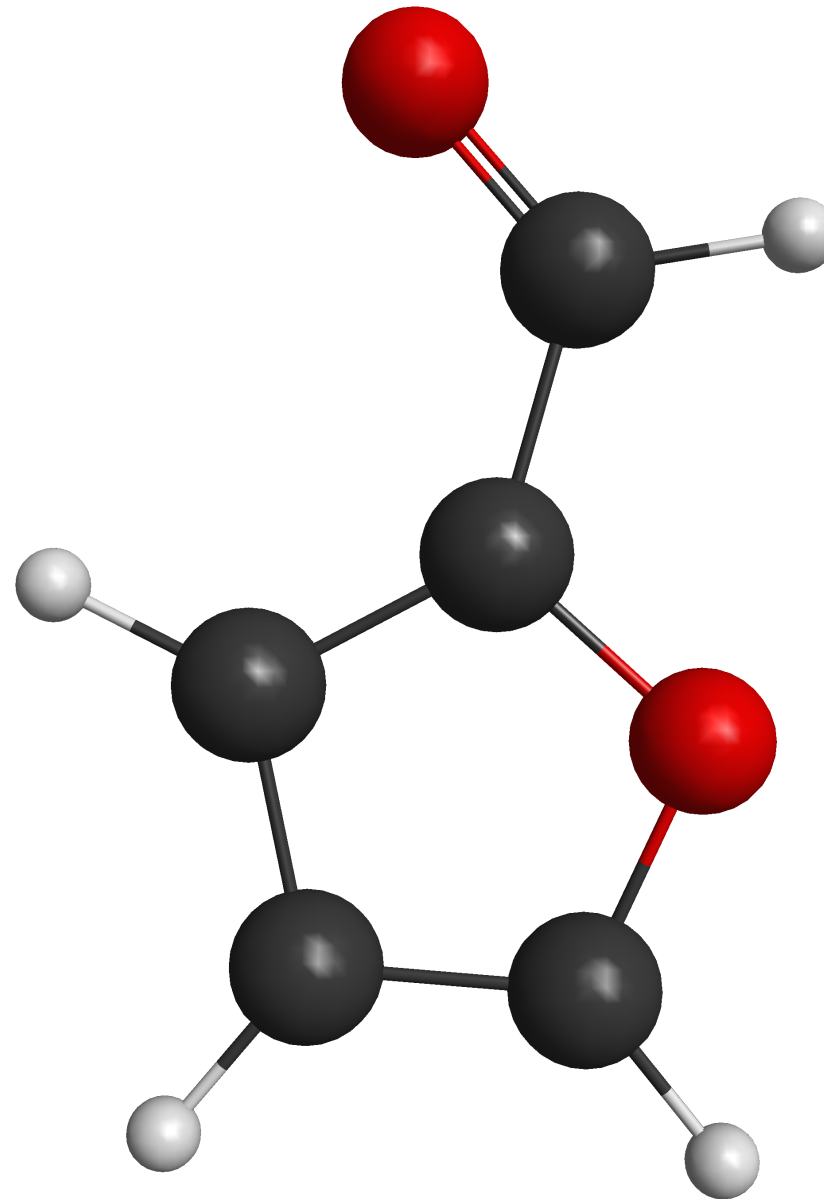
How this big change, caused by multichannel effects, in the ICS would affect modeling?

Multichannel effects on **total cross sections** for electron-phenol scattering

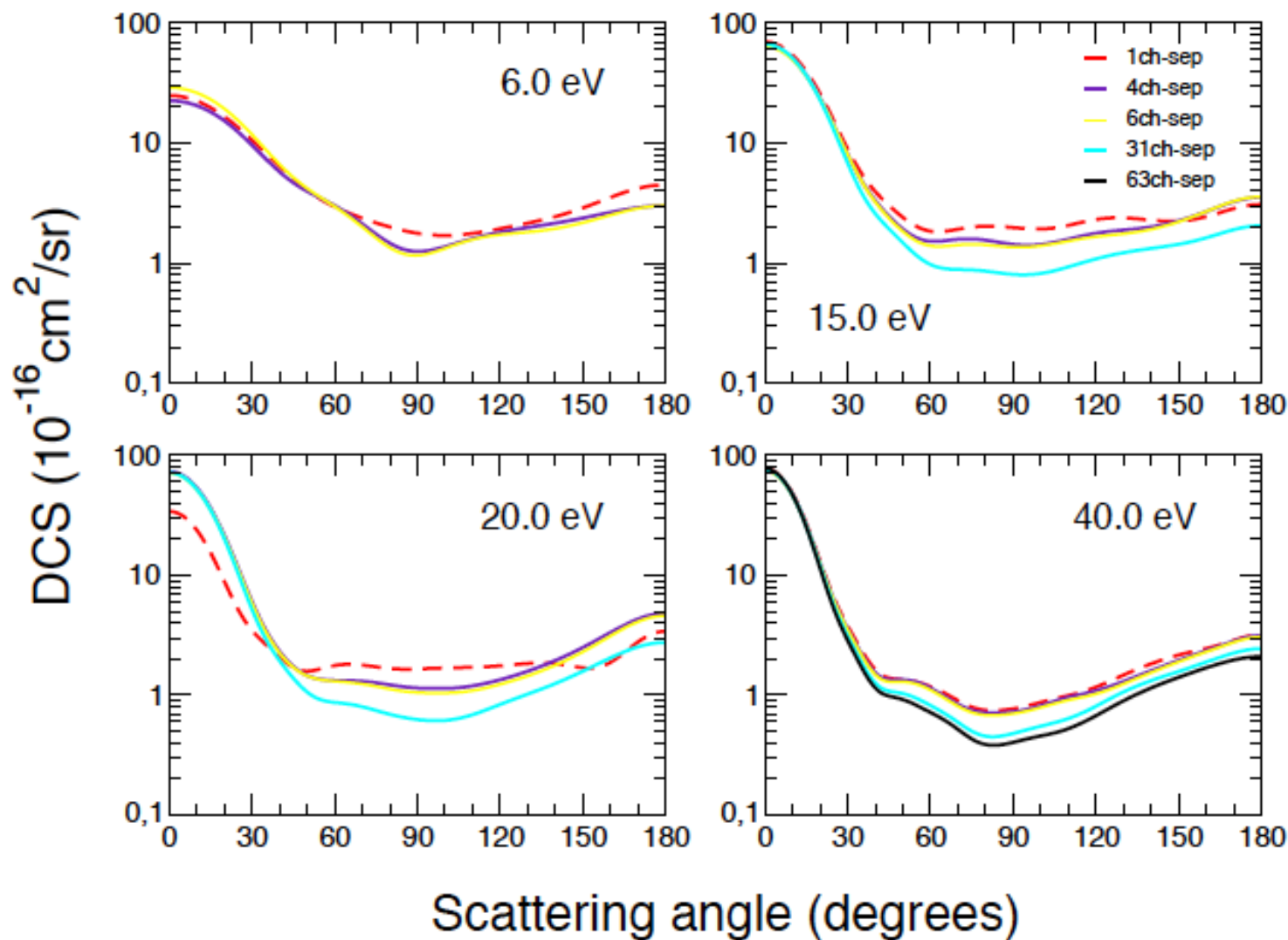


Note that the TCS in the 1ch-sep approximation is similar to the 33ch-sep case. This supports the flux competition picture.

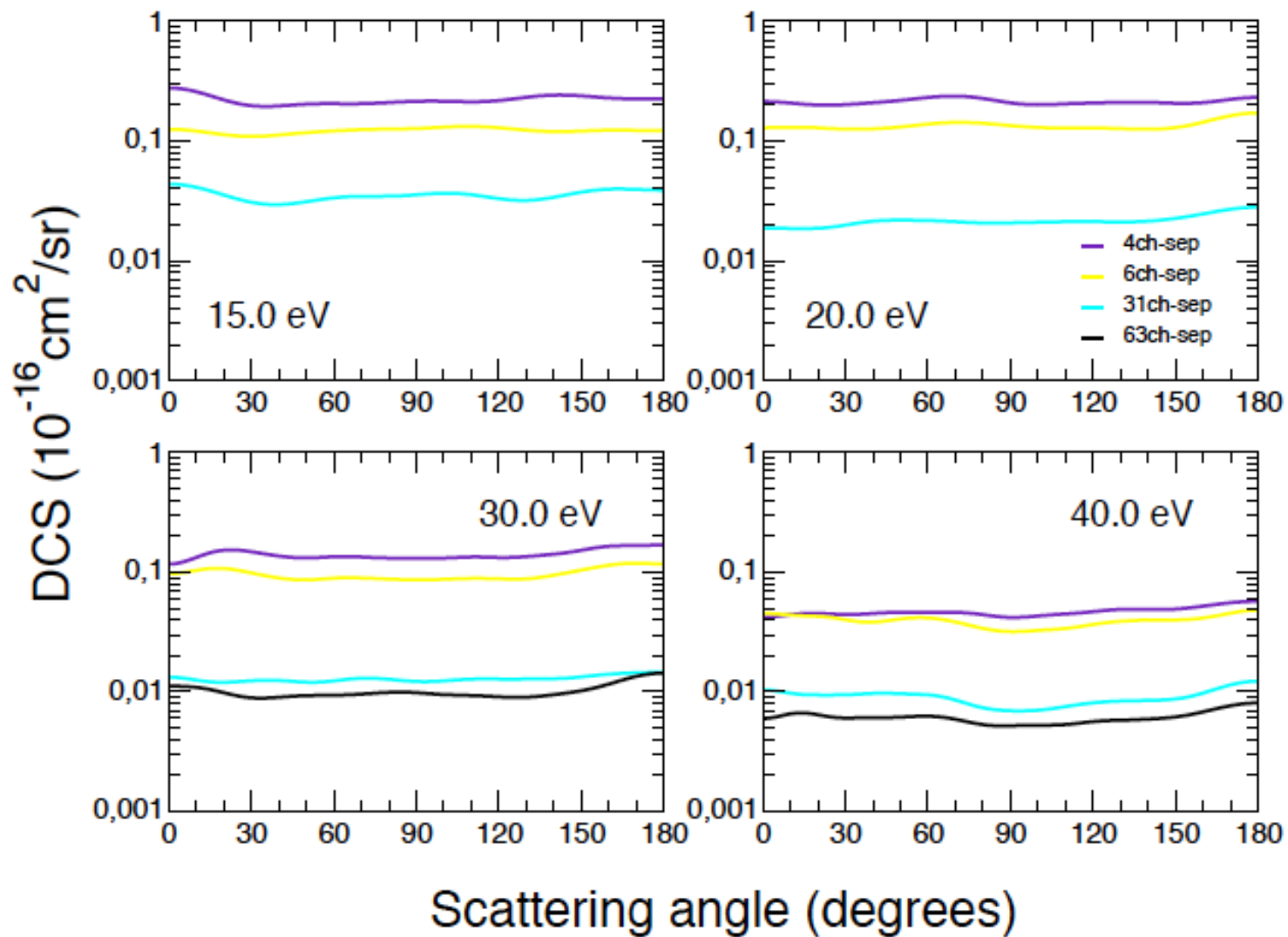
Electronic excitation of furfural by electron impact



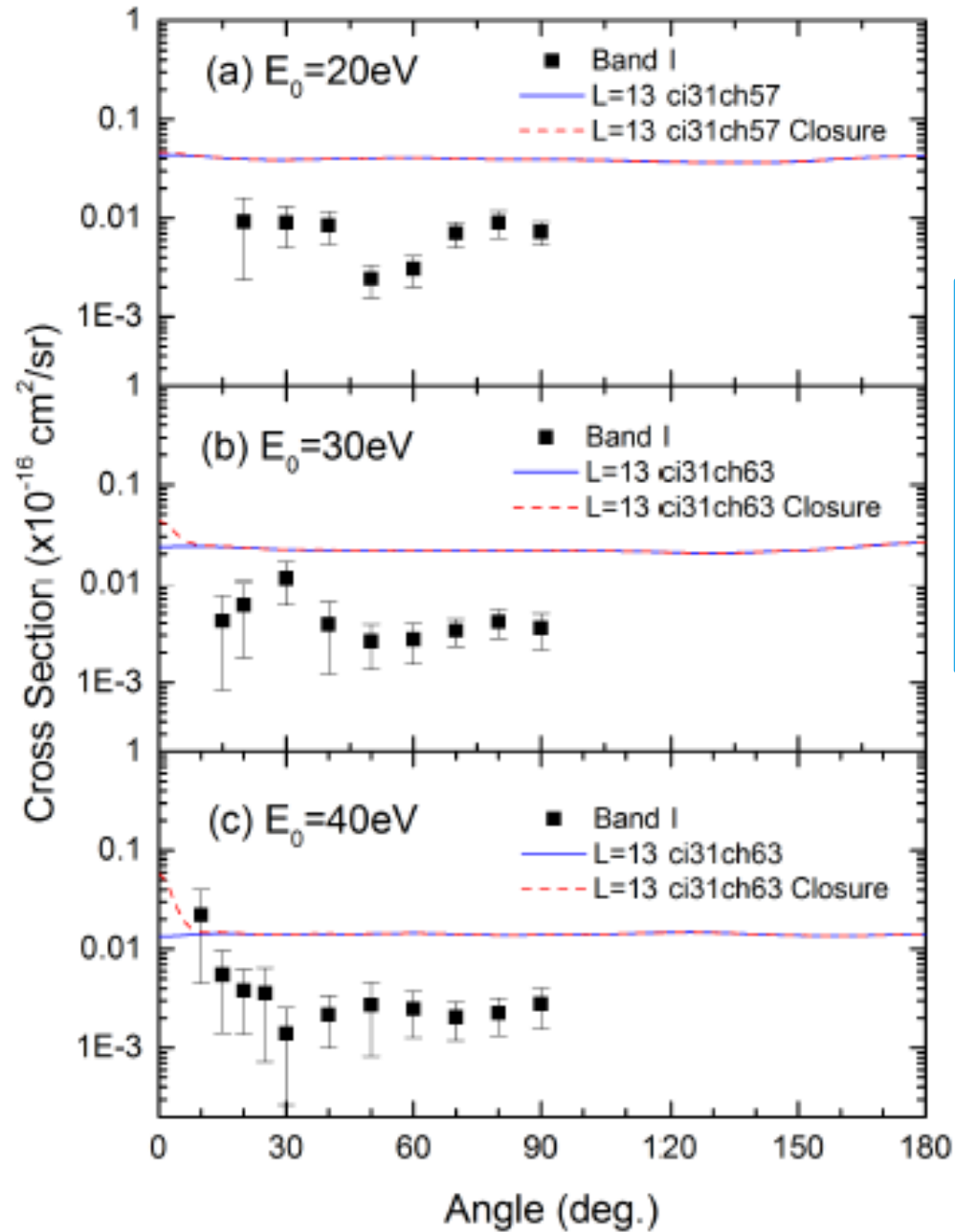
Electronic excitation of furfural by electron impact: Effects on the Elastic channel



Electronic excitation of furfural by electron impact: Effects on the first triplet state channel

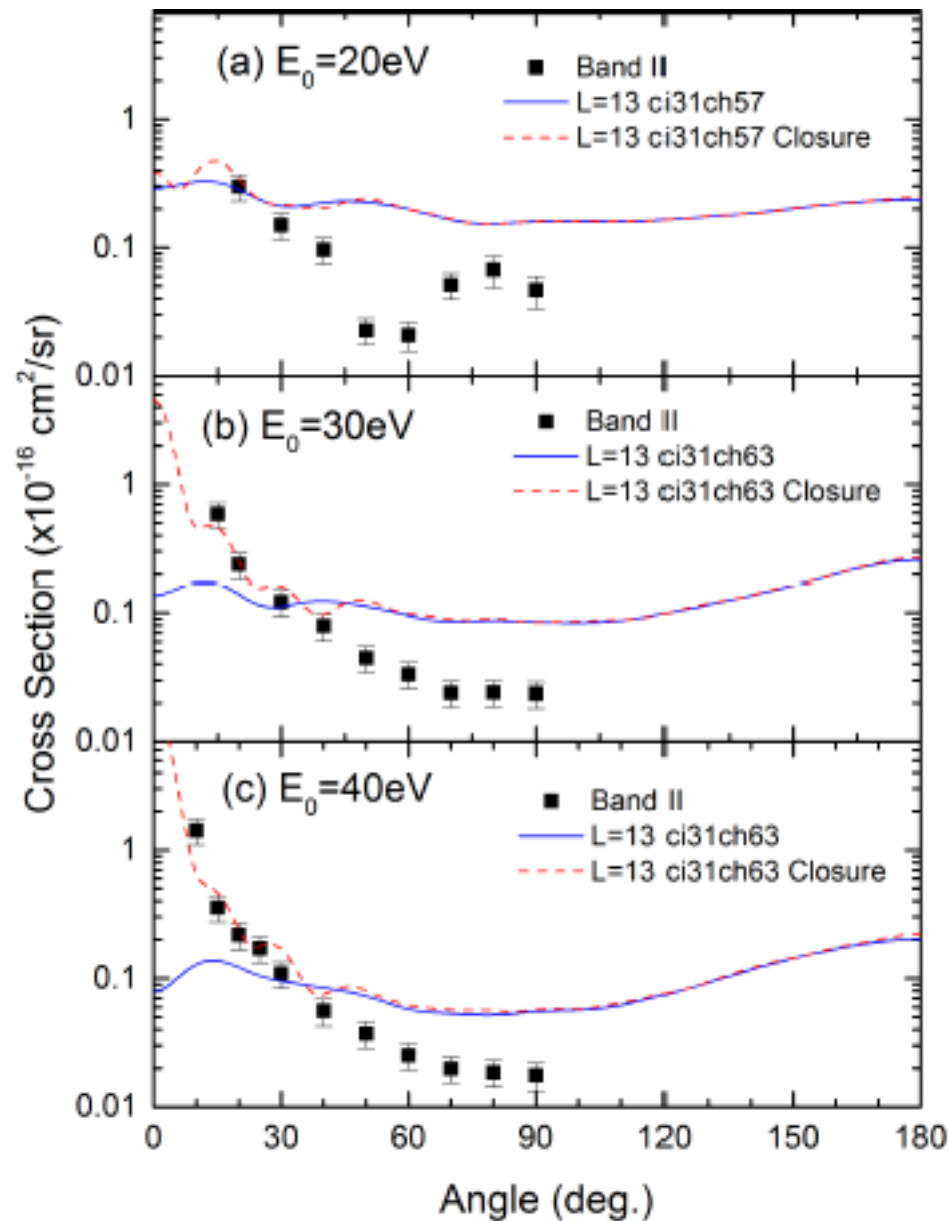


Electronic excitation of Band I of furfural by electron impact:



A factor of 3 difference between theory and experiments. Is it good?

Electronic excitation of Band II of furfural by electron impact:



The DCS at lower angles is dominated by the 1st Born approximation (which may work fine). Higher angles is a factor of 3 to 5 different. Is it good?

CONCLUSION

We (from the basic science community on electron-molecule scattering) justify our research on very important and (in some cases) very profitable applications. We have to work closer to plasma modelers in order to assess the quality and importance of our data (theory and experiment).

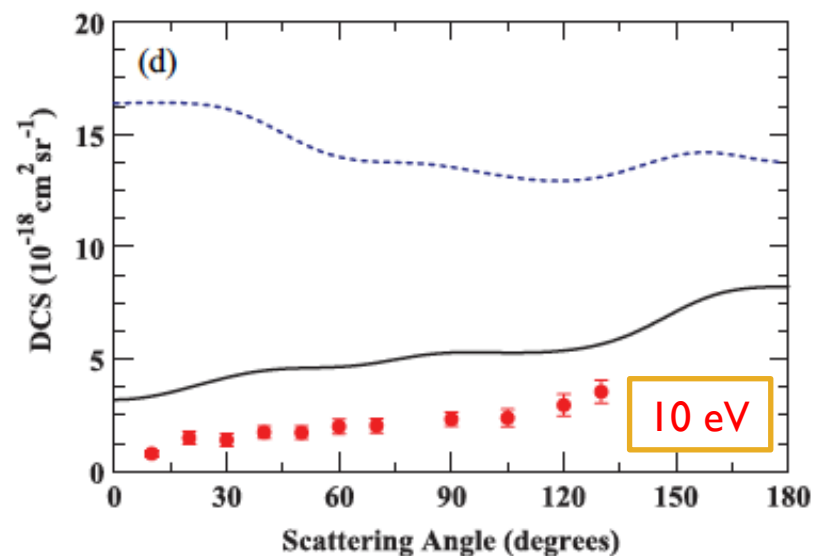
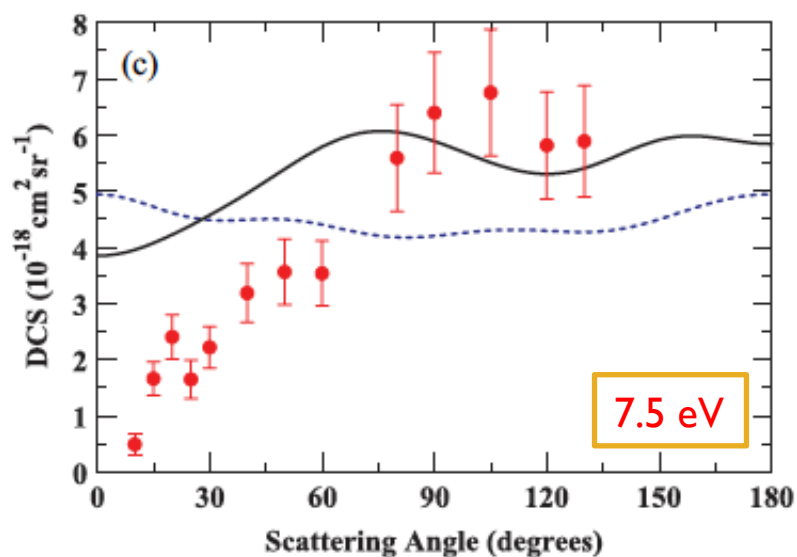
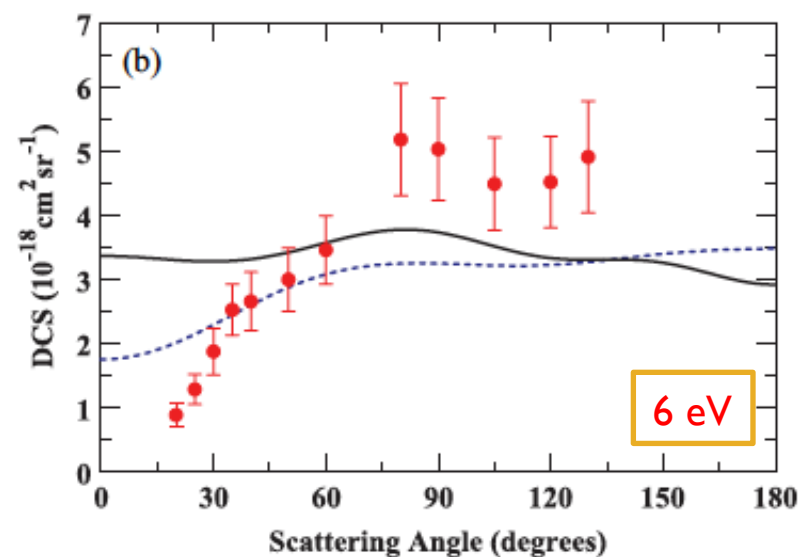
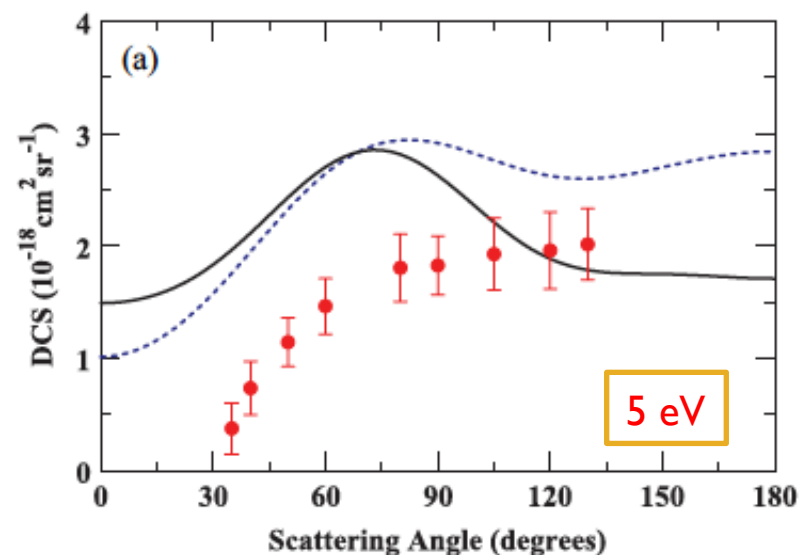
Thank you very much for your attention

A copy of this presentation is at

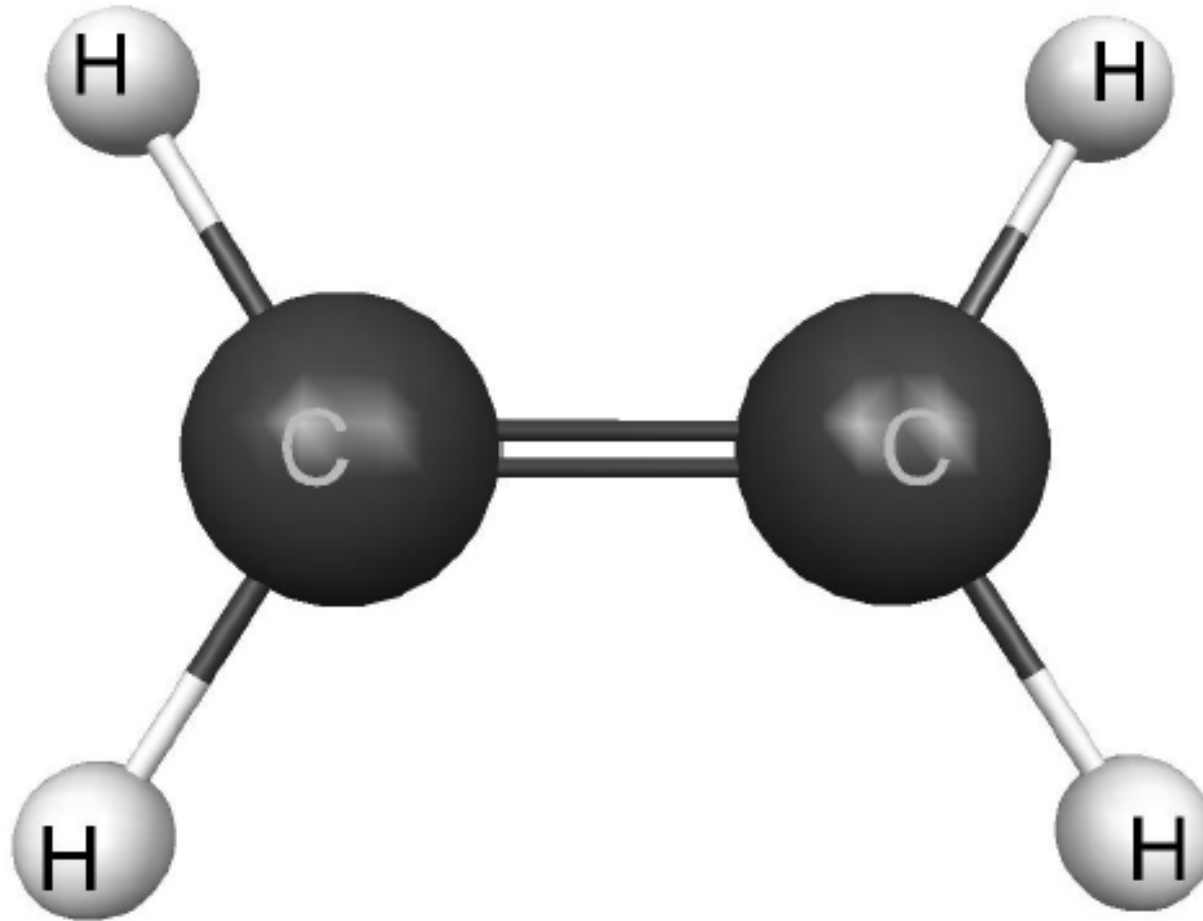
<http://www.ifi.unicamp.br/~maplima/maplima-GEC-Honolulu.pdf>

All the authors of the papers presented here are co-authors of this presentation

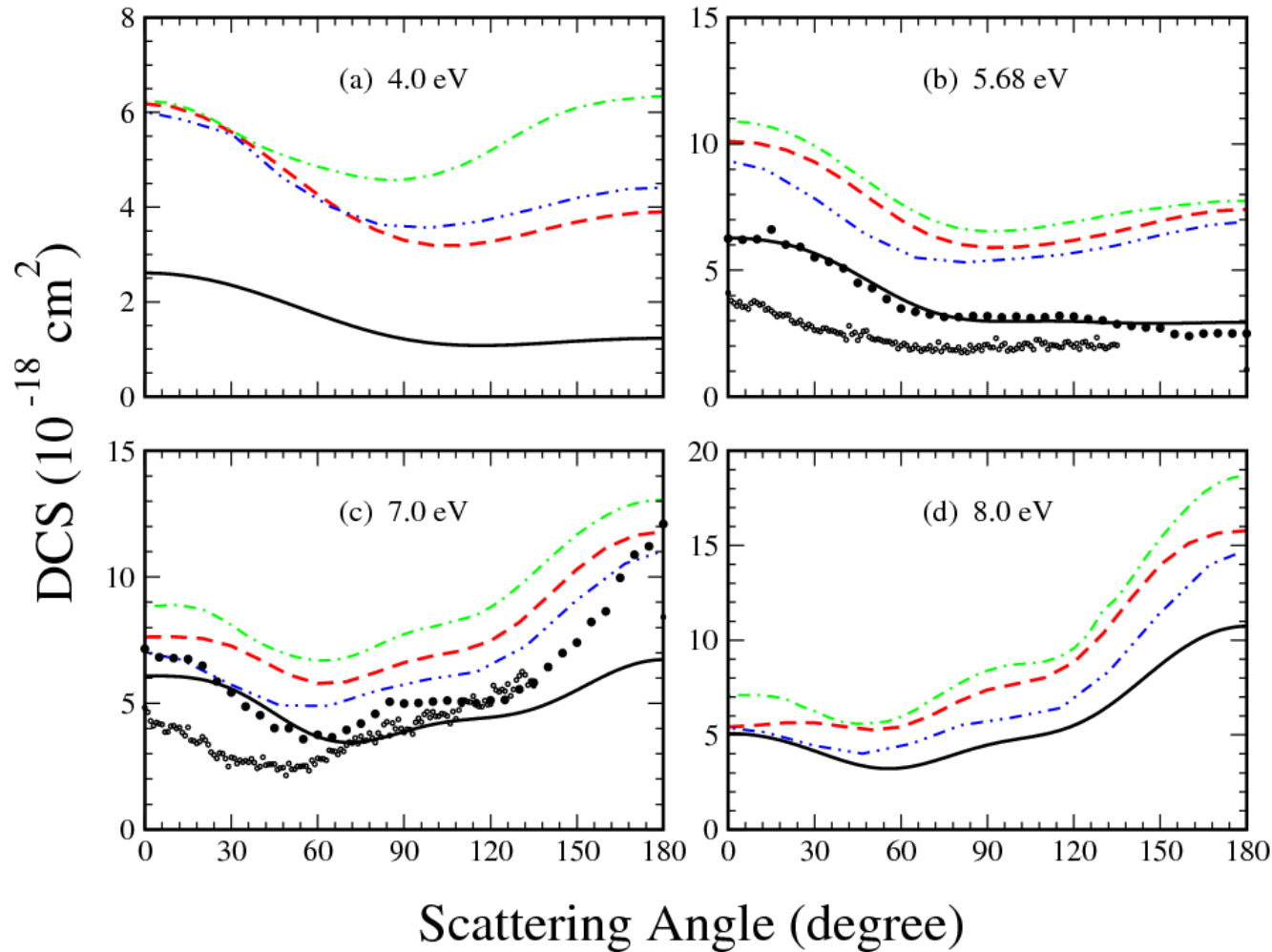
Electronic excitation cross sections of the 1st triplet state of furan



Electronic excitation of \tilde{a}^3B_{1u} state of C_2H_4 by electron impact



Electronic excitation of \tilde{a}^3B_{1u} state of C_2H_4 by electron impact



Color lines are 2-channel (close-coupling) results.

Black line are proper balanced n-channel coupling plus polarization effects.

Bullets are Michael Allan's experiments.

Surprisingly, at higher energies the agreement is not good!!

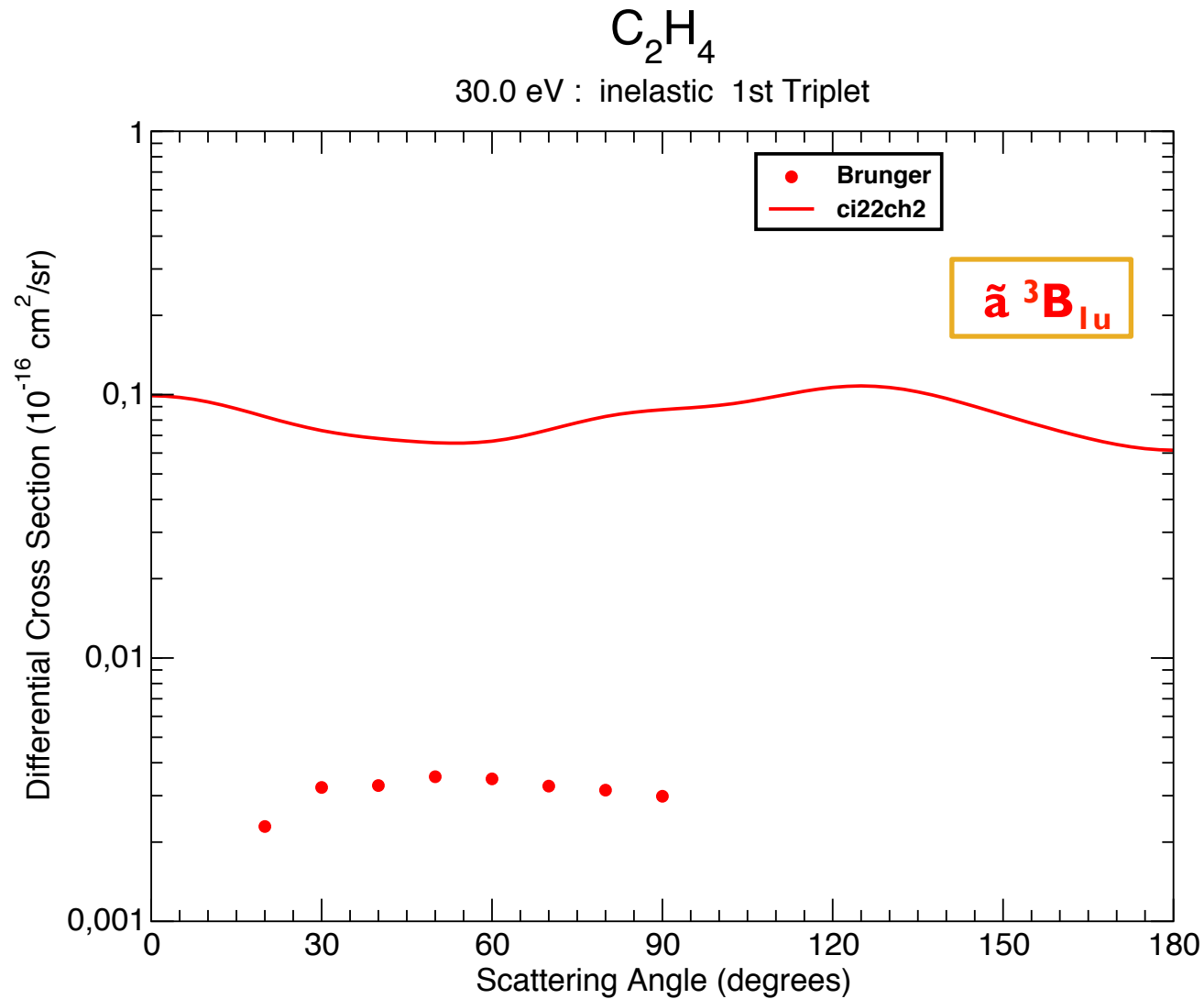


TABLE I. Calculated and experimental excitation energies for ethylene. Up to 20, 30 and 50 eV, the FSCI spectrum is composed by 138, 260 and 402 electronically excited states, respectively. The MOBSCI calculations at these energies were performed with 45 excited states, where 17 of them are physical excited singlets or triplets states and the others are pseudostates.

	Energy (eV)		
	FSCI	MOBSCI	Expt.
TRIPLET	3.56	3.60	4.36 ^a
	6.90	6.92	6.98 ^a
	7.73	7.75	7.79 ^a
	8.48	8.83	8.15 ^b
	8.80	9.08	8.57 ^b
	9.06	9.19	
	9.42	9.58	
	9.48	9.73	
	9.54	9.74	
SINGLET	7.11	7.13	7.11 ^b
	7.83	7.85	7.80 ^b
	7.88	8.55	7.90 ^b
	8.99	9.28	8.28 ^a
	9.24	9.37	8.62 ^b
	9.25	9.54	8.90 ^{a,b}
	9.63	9.71	9.10 ^a
			9.33 ^a
			9.51 ^{a,c}
		9.62 ^a	

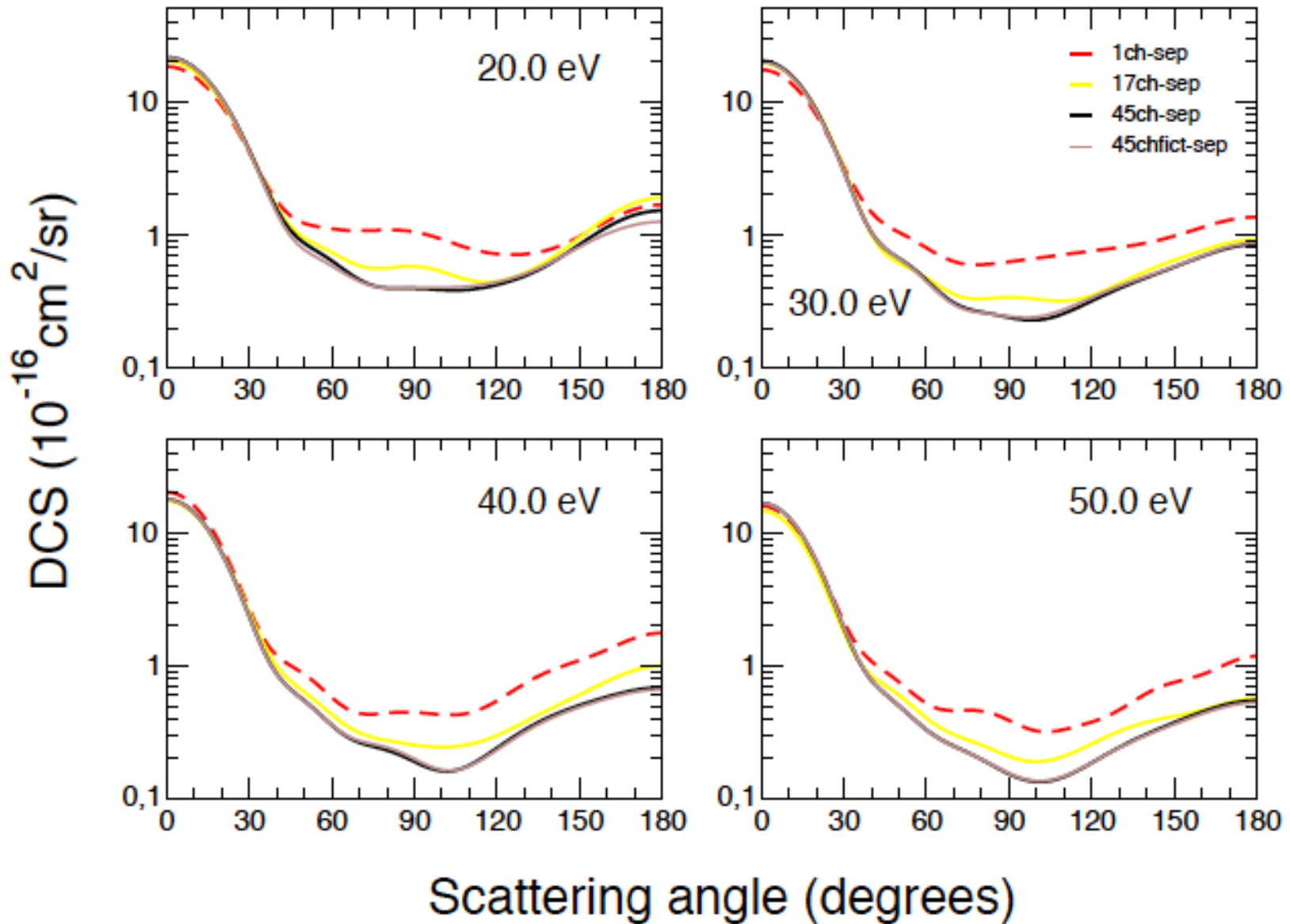
^a Experimental data from Ballard *et al.* [24].

^b Experimental data from Do *et al.* [16].

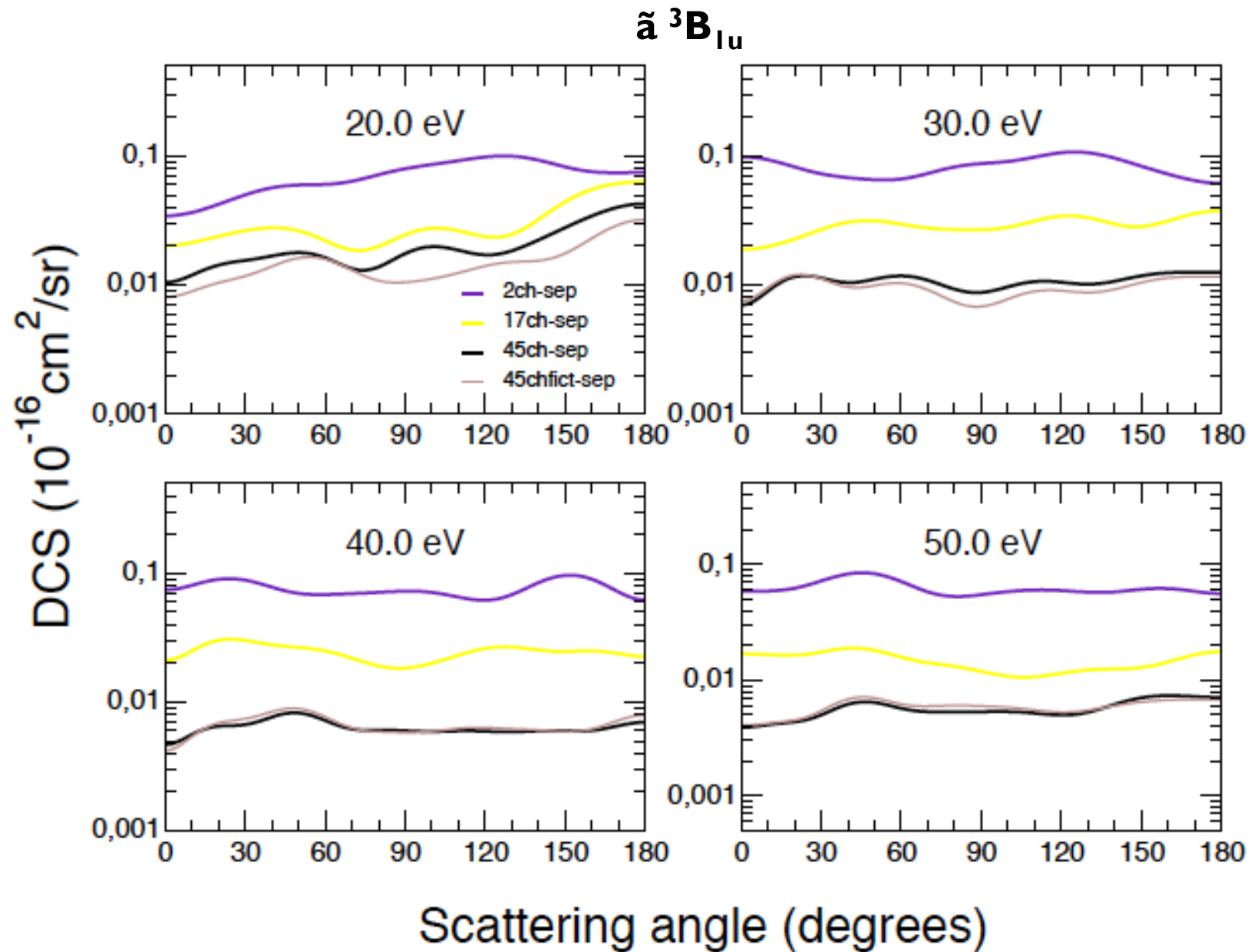
^c For this energy were found two states.

Only 22 pairs
Hole-particle

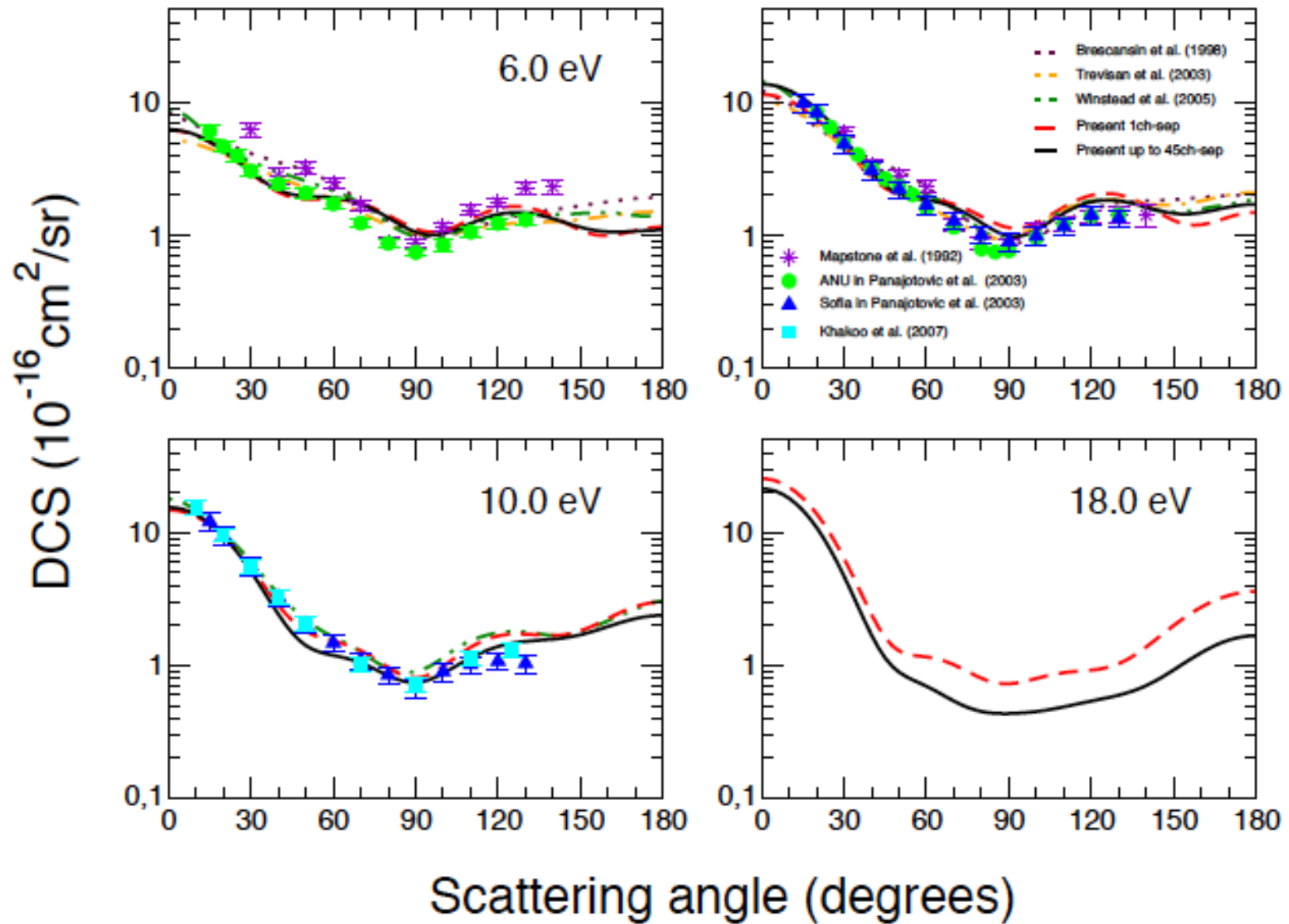
Flux dynamics in the elastic channel for e^- - C_2H_4 scattering



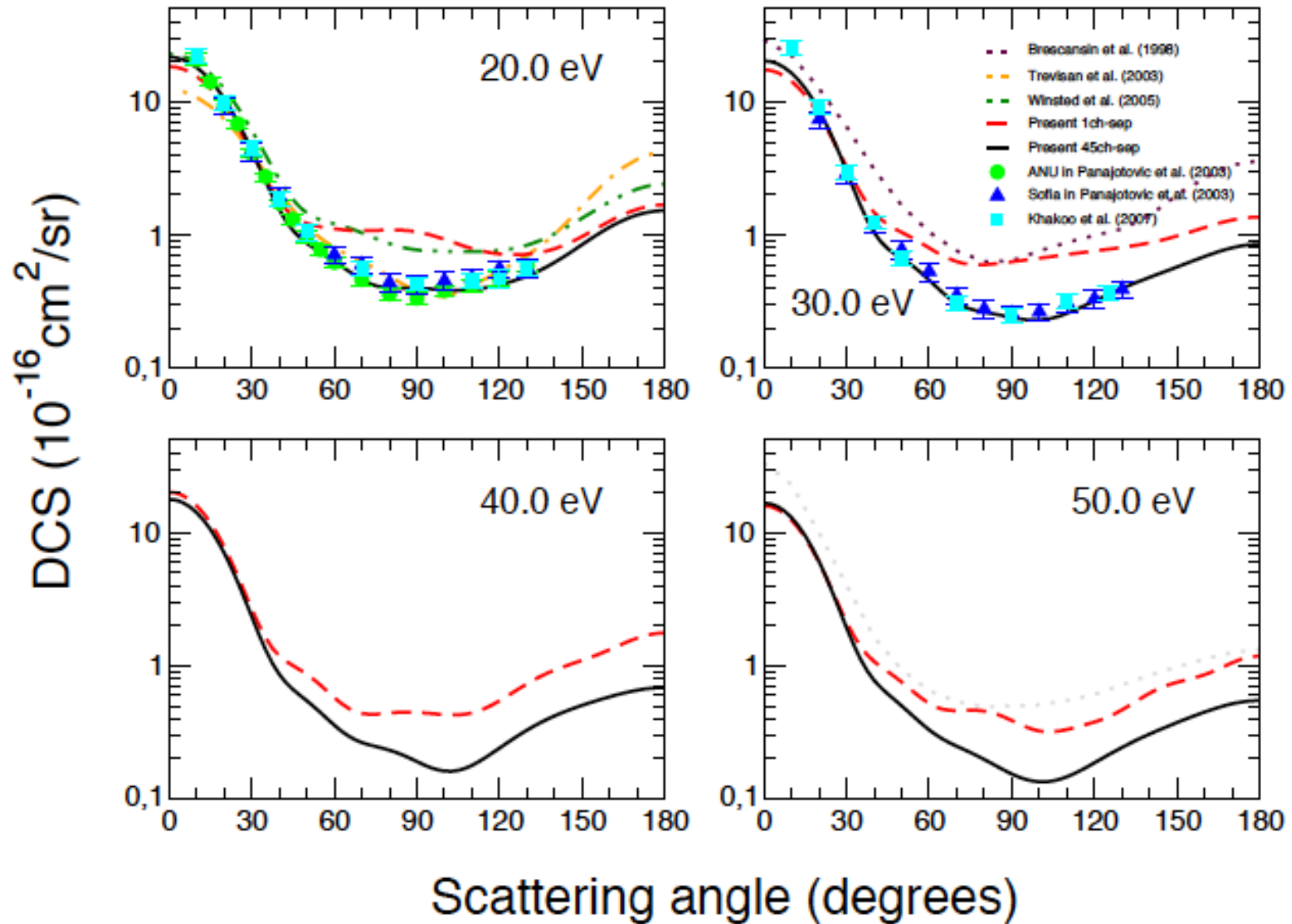
Flux dynamics to the (1st triplet) inelastic channel for e⁻-C₂H₄ scattering



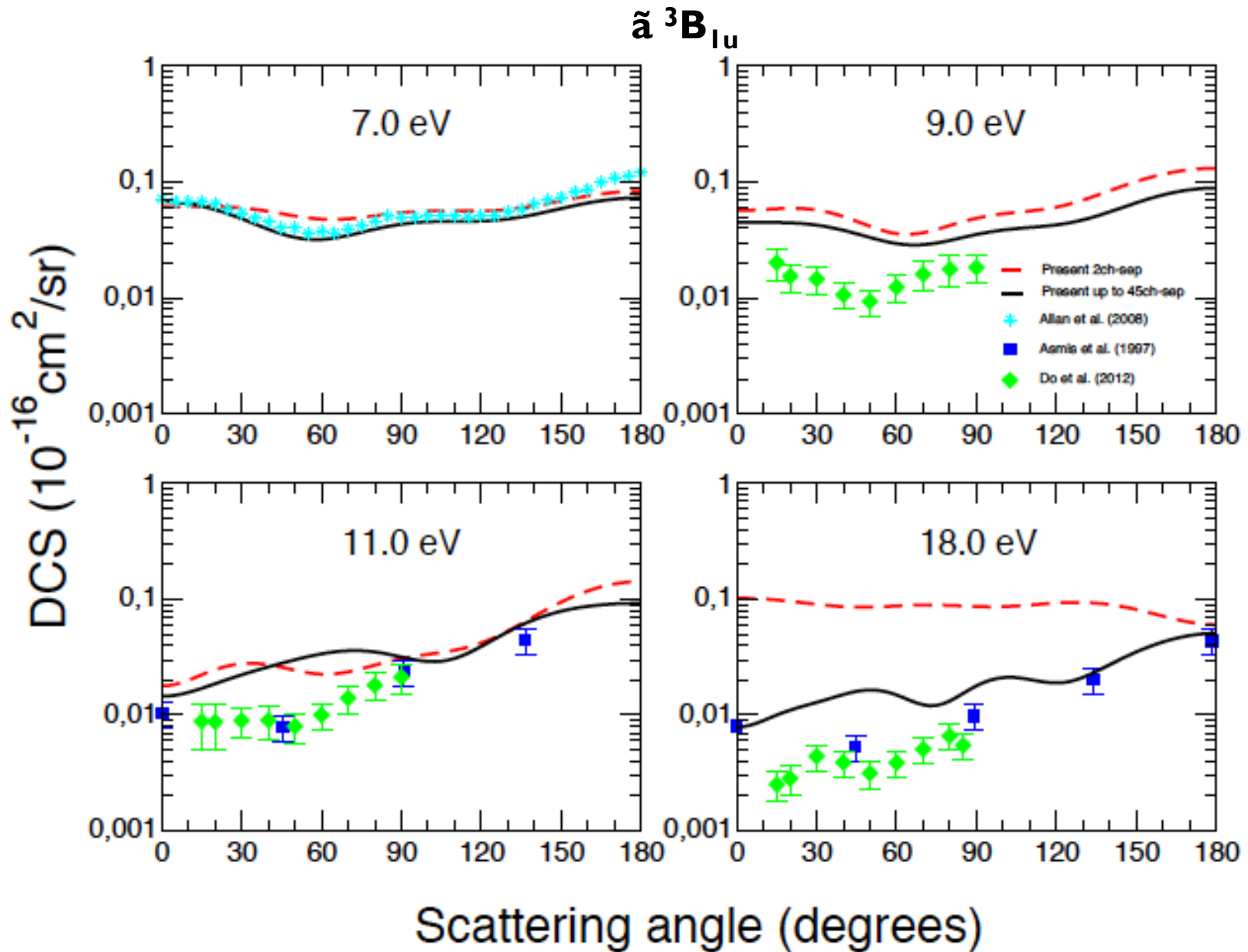
Elastic channel for lower energies in $e^-C_2H_4$ scattering



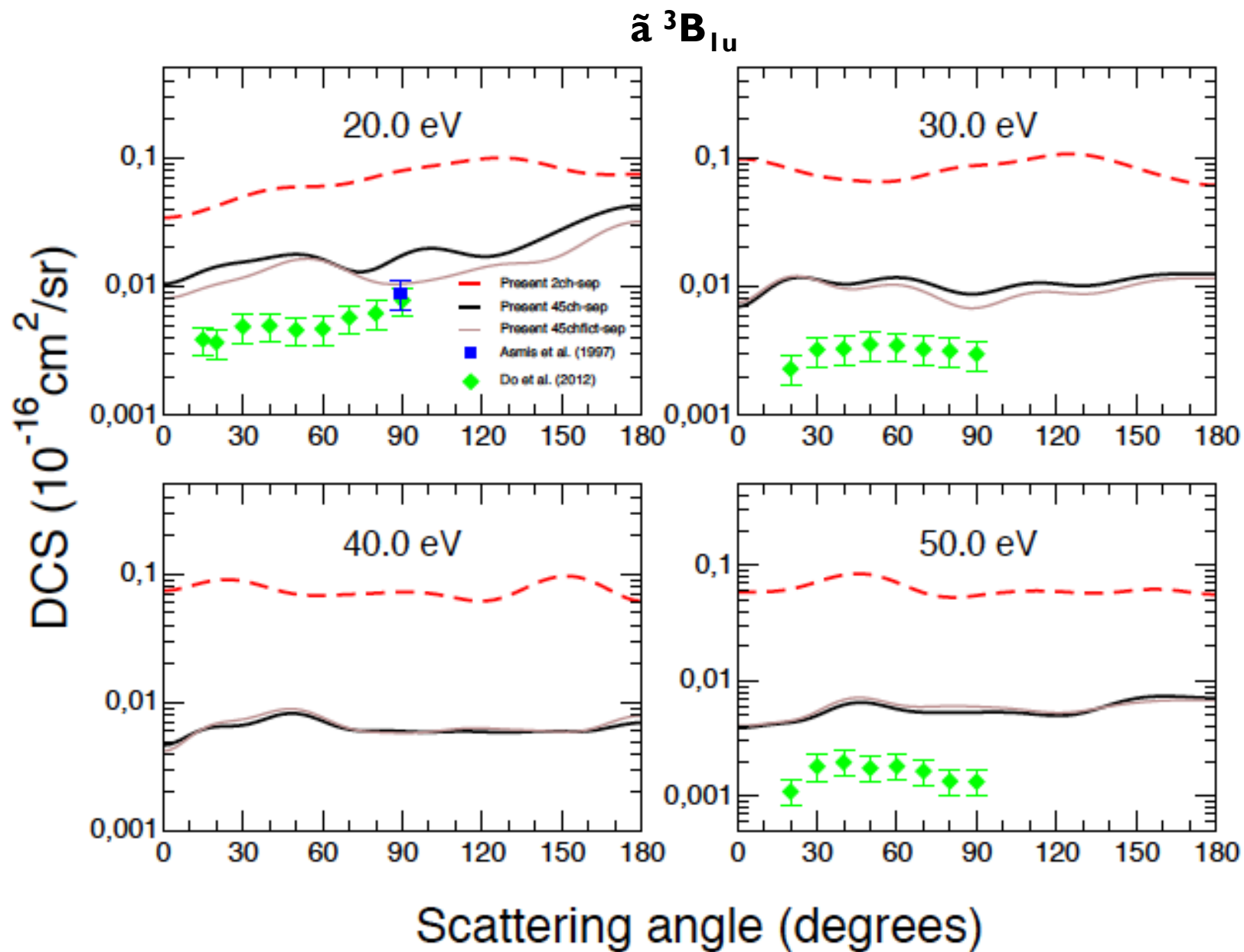
Elastic channel for higher energies in $e^-C_2H_4$ scattering



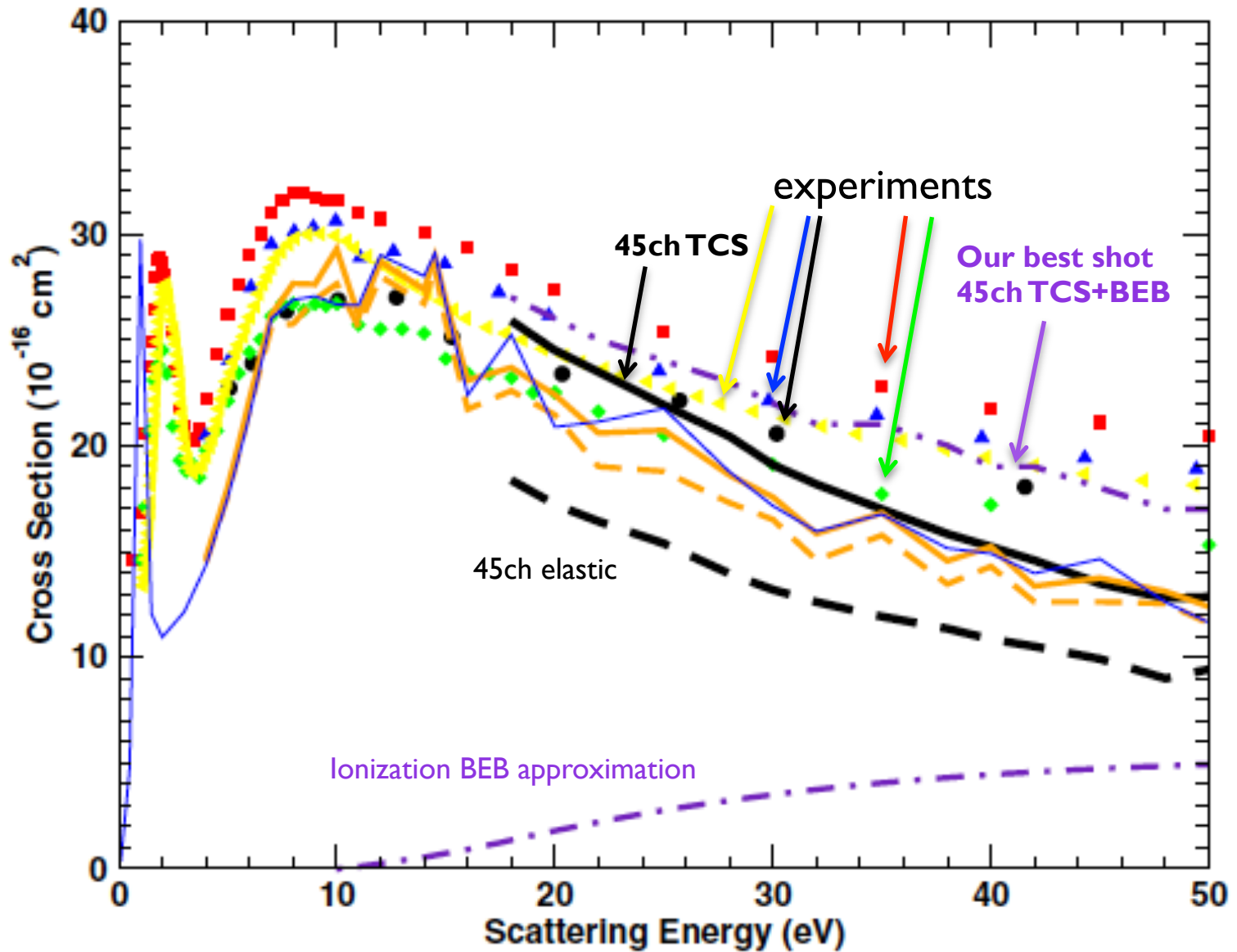
Inelastic channel (1^{st} triplet) for lower energies in $e^-C_2H_4$ scattering



Inelastic channel (1^{st} triplet) for higher energies in e^- - C_2H_4 scattering



Total cross section for e⁻-C₂H₄ scattering



Electron Collisions with Phenol...(H₂O)_n: search for microsolvation signatures in the DCS

